AD-A182 744 DETERMINATION OF ELECTRICAL PROPERTIES OF GROUNDING BONDING AND FASTENING..(U) SCIENCE AND ENGINEERING ASSOCIATES INC SEATTLE WA W W COOLEY APR 87 1/1

UNCLASSIFIED DOT/FAA/CT-86/8 DTFA03-84-C-00065 F/G 11/4 NL

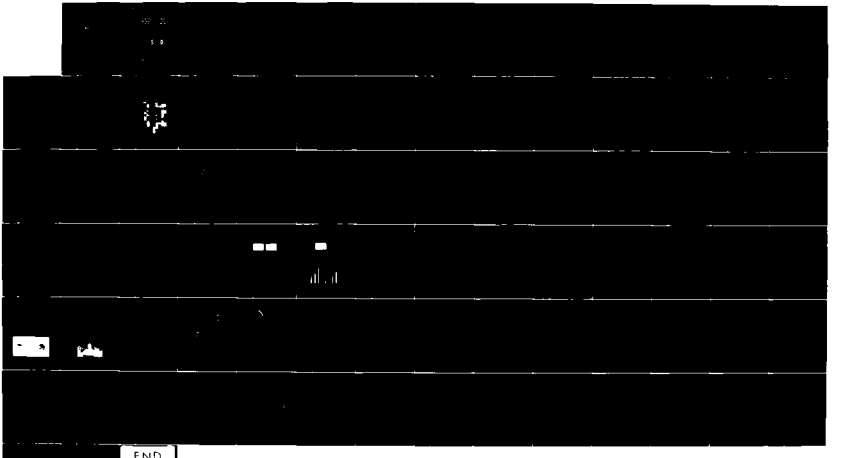

END
DATE FILMED
8

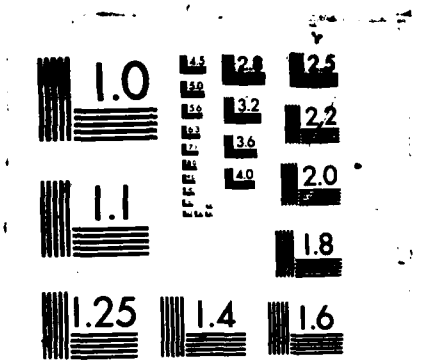

DOT/FAA/CT-86/8

FAA TECHNICAL CENTER
Atlantic City International Airport
N.J. 08405

Determination of Electrical Properties of Grounding, Bonding and Fastening Techniques for Composite Materials

William W. Cooley

Science & Engineering Associates, Inc.
701 Dexter Avenue N., Suite 400
Seattle, Washington 98109

April 1987

Final Report

U.S. Department of Transportation
Federal Aviation Administration

1. Report No.	2. Government Accession No.	3. Recipient's Catalog No.
DOT/FAA/CT-86/8		A182744

4. Title and Subtitle	5. Report Date
Determination of Electrical Properties of Grounding, Bonding, and Fastening Techniques for Composite Materials	April 1987
	6. Performing Organization Code
7. Author(s)	8. Performing Organization Report No.
William W. Cooley	
9. Performing Organization Name and Address	10. Work Unit No. (TRAIS)
Science and Engineering Associates, Inc. 701 Dexter Avenue North, Suite 400 Seattle, WA 98109	11. Contract or Grant No. DTFA03-84-C-00065
12. Sponsoring Agency Name and Address	13. Type of Report and Period Covered
Federal Aviation Agency Technical Center Atlantic City International Airport, NJ 08405	Final Technical Report September '84-December '85
	14. Sponsoring Agency Code

15. Supplementary Notes

16. Abstract

This report documents the results from a limited study of Electrical Parameters of Composite Materials. These efforts provided an evaluation of grounding and bonding test methods for metal, metal honeycomb, and advanced composite materials. A review of the electrical currents in the bonding and grounding paths on aircraft concluded that the lightning environment is the most severe followed by power system faults and on-board HF radio. It is recommended that the conventional 2.5 milliohm grounding and bonding requirement may be relaxed providing that special tests are conducted on the structure and subassemblies that enter into the grounding and bonding current paths. These tests are defined and recommendations made for advanced structures. A limited analysis of published test results concluded that good agreement may be possible between predicted values and test results for complete structures, subassemblies, and components.

17. Key Words	18. Distribution Statement
Composite Materials; EMI; Lightning; Electrical Parameters; Grounding; Bonding	This document is available through the National Technical Information Service Springfield, Virginia 22161

19. Security Class. (of this report)	20. Security Class. (of this page)	21. No. of pgs.	22. Price
Unclassified	Unclassified		

Form DOT F 1700.7 (8-72)

PREFACE

This report was prepared by Science and Engineering Associates, Inc., (SEA) under Contract No. DTFA03-84-C-00065 with the Federal Aviation Administration (FAA) Technical Center, Mr. David Lawrence was the contracting officers technical representative.

SEA's program manager has been Dr. William W. Cooley. The analyses were performed by Dr. Barbara G. Melander with technical support from Deb Shortess.

TABLE OF CONTENTS

LIST OF ILLUSTRATIONS

LIST OF ILLUSTRATIONS (Continued)

LIST OF TABLES

LIST OF TABLES (Continued)

LIST OF ACRONYMS

EMI	Electromagnetic Interference
RF	Radio Frequency
FAA	Federal Aviation Administration
NASA	National Aeronautics and Space Administration
EM	Electromagnetic
ASD	Air Force Aeronautical Systems Division
AFWAL	Air Force Wright Aeronautical Laboratories
SAMSO	Air Force Space and Missile Systems Office
HF	High Frequency
LF	Low Frequency
SAE	Society of Automotive Engineers
AEHP	Atmospheric Electricity Hazards Program
gr/ep	Graphite Eposy
EMC	Electromagnetic Compatibility
TTL	Transistor-to-Transistor Logic

EXECUTIVE SUMMARY

This report presents an analysis of the electrical properties of the advanced structural materials being applied for the next generation of general aviation and transport aircraft. The materials considered include aluminum honeycomb, bonded aluminum, graphite epoxy and kevlar.

There have been concerns expressed in the literature regarding the grounding and bonding specifications for present aircraft structures not being achievable for newer materials. The technology base for these materials was reviewed for electrical properties, test procedures and test data. Data is presented that confirms many of the concerns that adequate grounding and bonding may not be achievable using these materials under the constraints of present specifications limits.

The analysis presented re-evaluates the basis for the present 2.5 milliohm grounding and bonding specification limits with the conclusion that the present limit may be too low a value for application to an entire aircraft. This analysis included an assessment of the full range of grounding and bonding system EM environments applicable to aircraft and aircraft electrical/electronic equipment. It also considered estimated currents from lightning strikes, power system faults, RF current returns from on-board and near-by transmitters, and the normal operating currents from avionics and electrical equipment. Estimates of the tolerance of on-board systems to ground system voltages were made indicating the severity of effects from the various current sources. The results of this assessment provide an estimated range of allowable grounding and bonding limits for each of the current sources. The most severe threats to equipment are from lightning currents. The next most severe threats are from power system faults, on-board radio transmitters and electrical equipment having ground returns. If the 2.5 milliohm specification were applied, the assessment indicates that all systems would be safe.

For many of the new materials being applied, the structure will be far more resistive than the present 2.5 milliohm requirement. Kevlar is an insulator and graphite/epoxy structures may have resistances on the order of a few ohms. Designs using these materials will require special attention to allow the addition of enough metal such that protection against lightning strikes may be achieved. Special attention will also be required to add metallic pathways in the grounding and bonding system so that on-board systems will function properly in the presence of currents anticipated from normal or fault conditions in on-board equipment.

Test requirements are reviewed to develop and verify designs needed for the basic structure and equipment grounding systems in aircraft structures where a 2.5 milliohm requirement cannot be met. The real hazard to aircraft safety from inadequate grounding and bonding is from arcing, sparks and hot spots in fuel and fuel vapor areas. Available test methods are presented and reviewed with particular emphasis on protection against a fuel system hazard. Recommendations are provided regarding a range of tests needed for the complete airframe, subassemblies, and small samples or test coupons of joints from various portions of a structure. For fuel and fuel vapor areas, tests are needed to determine allowable maximum limits of current in each structural

joint so that hot spots or sparks will not be formed. This problem is approached by first testing samples of each type of joint for maximum allowable current limits. Tests are then conducted on the complete structure, or major portions of structure such as a wing, to determine the currents from lightning or power system faults. From these two tests an assessment may then be made to validate that the design will be spark free.

The final portion of this study evaluated the role of analysis in grounding and bonding design verification. If successful, an analysis effort could be useful in reducing the extent of complete vehicle testing needed for design verification. There is little reference in the literature to applications of EM theory to the analysis of sparking or hot spots in materials or in joints between various materials. An analysis of existing test data is presented to evaluate an ability for prediction of sparking levels for three different joining methods in graphite epoxy structure. Predictions are also presented for voltage breakdown of bonded aluminum structures. Comparisons of these analysis results with published test data indicate that these analysis methods are promising and that further work should be done on a wider range of fastening methods and materials. Since the spark thresholds of joints depends strongly upon specific sealant materials and fastening technique, analysis is not expected to ever replace testing of joint samples. Analytical modeling methods are described that may be useful in predicting current flow in a complete structure. The technique is applied to predicting the currents in a graphite epoxy wing; the results are very favorable. This technique could be very useful for demonstrating that a complete structure is spark free, given the maximum current limits for spark free joints and thereby reducing the need to test every joint in the complete structure.

SECTION I - INTRODUCTION

PURPOSE AND SCOPE.

Purpose. Science and Engineering Associates, Inc. prepared this report as part of a study program for the Federal Aviation Administration entitled "Composite Material Electrical Properties Analysis." This limited study was to: a) provide an evaluation of grounding and bonding test methods for metal, metal honeycomb and advanced composite materials; b) select candidate bonding and grounding systems for modeling, test and evaluations; c) perform analysis of selected test techniques; and d) provide recommendations based upon the analysis. It is expected that new requirements and design guidelines will be needed for the advanced composite structures.

Background. Competition in the marketplace for aircraft sales and the high cost of fuel is developing pressure on manufacturers to use advanced technology materials and electronic equipment in the next generation of aircraft. This is evident both in large transport and in general aviation aircraft currently under development. Several general aviation aircraft employing advanced technology are nearing, or are in, the certification process including the Beech 'Starship', Learfan and AVTEK. In addition to the all-electric engine control for the Boeing 757, transport aircraft manufacturers are researching the use of advanced composite structures, digital data buses (beyond ARINC 429), and all-electric flight control systems.

Among the advanced structural materials and processes being applied are (1) composite materials to obtain higher strength to weight ratios, and (2) metal-to-metal bonding with adhesives in place of fasteners and rivets to obtain smooth outer surfaces and reduced drag. Completely non-metallic structures are also being developed, using such materials as bonded honeycomb, kevlar, fiberglass, and graphite/epoxy. The new structural fabrication methods also reduce manufacturing costs. Other advantages include reduction in corrosion and fatigue.

Scope. This report provides technical data on bonding and grounding requirements for composite materials and recommendations for bonding and grounding specifications applicable to advanced technology aircraft such as typified by 1) the Pratt & Whitney 2037 all-electric-controlled engines currently being installed on the Boeing 757 and, 2) the all-composite airframe and newly designed digital flight control and data bus currently being developed for the Beech 300A 'Starship'. Because of the low conductivity of the composite materials and the nonconductive adhesive bonding materials, lightning and Electromagnetic Interference (EMI) are more severe threats than they were for previous all metal aircraft. Hence, these two aircraft, and future ones as well, require new specifications and qualification test techniques to control the bonding and grounding of the structure and the electrical & electronic radio frequency (RF) current return circuits.

Study Description. An overview and Task Flow for the reported work is shown in Figure 1. These activities were aided by earlier work including lightning technology developed by the Federal Aviation Administration (FAA), National Aeronautics & Space Administration (NASA), Navy, Air Force, Army and Defense Nuclear Agency (DNA).

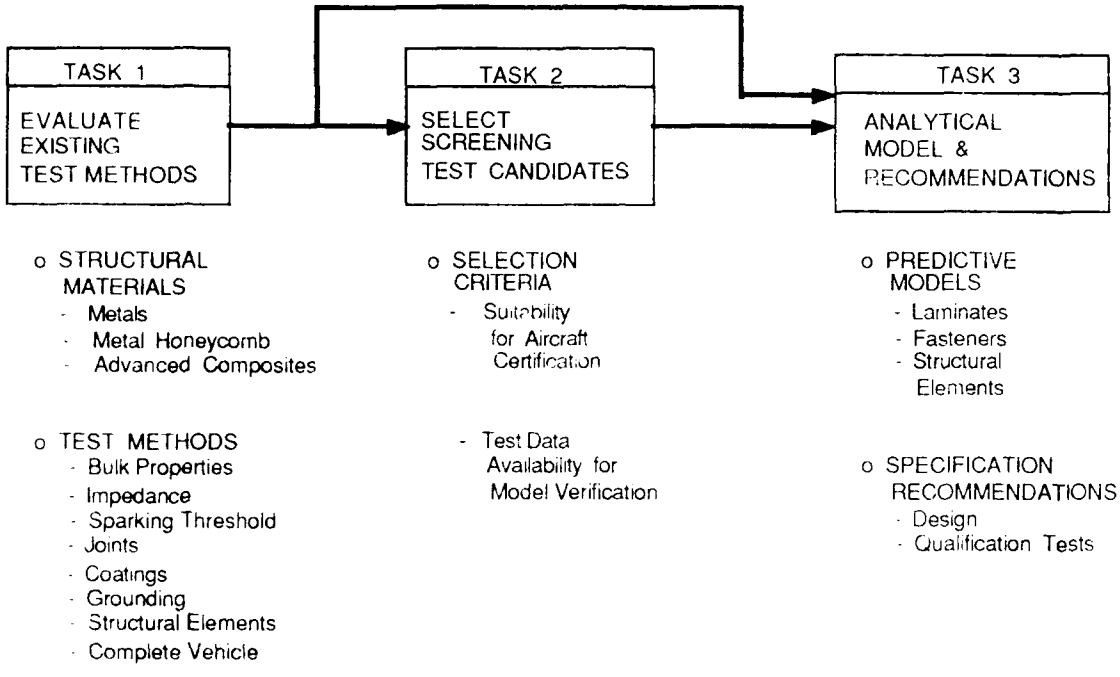

FIGURE 1. COMPOSITE MATERIAL ELECTRICAL PROPERTIES ANALYSIS - TASK FLOW

EM EFFECTS ON COMPOSITE MATERIALS.

EM Potential Protection Problem. There are several potential problems preventing widespread use of the new structural technology. These include the variability of the mechanical and electrical parameters, impact strength, effects of environmental factors, production controls, lightning protection, static electrification, and electromagnetic compatibility.

The trend in avionic/electrical equipment toward digital circuits having lower operating voltage and power levels adds to the concern regarding lightning and static electrification protection. The poor (i.e. lower) conductivity of the new materials and the bonds between structural members makes it difficult to obtain the 2.5 milliohm bonding and grounding required by current military specifications (MIL-B-5087). This bonding value is thought to provide sufficiently low voltages between different parts of the electrical system when the aircraft is struck by lightning.

There are also concerns about potential interference between different on-board digital systems and sources of EMI. The Electromagnetic (EM) shielding provided by a graphite composite fuselage, without seams or joints, is one to two orders of magnitude smaller than that provided by a conventional aluminum fuselage. Seams and joints reduce the shielding to a practical upper limit of 25 to 40 dB depending on size and number of seams and joints. Finally, EM compatibility between digital and RF circuits using the structure as a return path is also of greater concern than for prior aircraft.

Considerable effort will be required to adequately protect electronic systems in advanced aircraft structures. This is due to the reduced margins of safety between the EM induced transients (stress) and the ability of future technology equipment to withstand these transients (strain). Since advanced aircraft electronics operate at a few volts compared with a few tens of volts for older aircraft systems, the margins of safety may be further reduced in future systems.

Lightning and static electrification protection of aircraft and ground based systems has been the topic of considerable technical research and concern. During the last several years, there have been many conferences dedicated to this topic and considerable work completed (References 1-39). Because of the role of grounding and bonding in the overall electrical and electronic systems, this topic is also included.

AF Task Force Recommendations. In 1979 the US Air Force conducted an assessment of the potential electrical and electromagnetic effects created by widespread application of advanced composite materials to aerospace systems (Reference 5). Technical specialists from the Air Force Aeronautical Systems Division (ASD), Air Force Wright Aeronautical Laboratories (AFWAL), and the Air Force Space and Missile Systems Office (SAMSO) formed a working group that collected and analyzed responses from the government agencies and contractors involved in advanced composite research. Questionnaires were developed and sent out on the two composite materials predominantly used for aircraft -- graphite/epoxy (gr/ep) and kevlar. The graphite materials considered were GY-70 and T-300. The first has the higher conductivity and is primarily used for missiles. The second has slightly lower conductivity and is used in aircraft for its mechanical properties. Kevlar, essentially an insulator, has many aircraft, missile and spacecraft applications and is widely used on present

aircraft. Kevlar requires special treatments against static electricity and for use as an antenna ground plane.

The results of the survey (Reference 5) produced the following ranked list of concerns, which were a direct result of the differences in conductivity of the materials (relative to aluminum), shielding, and the joint impedances:

- o Lightning spark free fuel system designs
- o Lightning indirect or induced effects
- o Bonding of joints and seams
  - Corrosion control
  - Electrical durability
  - Structural integrity
  - Producibility
- o Power system grounding
- o High frequency (HF) and low frequency (LF) antenna performance
- o Combined space environment effects
- o Specific data on parametric values
- o Technology transition

The relative importance of these factors is summarized in Figure 2. This data clearly shows the importance of electrical properties of joint bonding, material conductivity and electrical grounding.

The study group also stated that technological development is essential in five major areas:

a. Electromagnetic shielding characterizations and standardization are necessary to provide electrical parameters for designs having universally accepted data.

b. Effective, durable, maintainable and producible electrically conductive joint technology is necessary to allow accurate designs characterization and eliminate many concerns regarding effects of joints on the EM shielding effectiveness.

c. A lightning proof fuel system is required. In addition to the usual problems of arcing and sparking, the problem of hot spot ignition is a major concern.

d. Design alternatives need to be defined and demonstrated to preclude power distribution loss and lightning induced transient problems with sensitive electronics and power system returns.

e. Because of the lack of data available, the effects of the space environment on the materials electrical and mechanical parameters and related design features require definition.

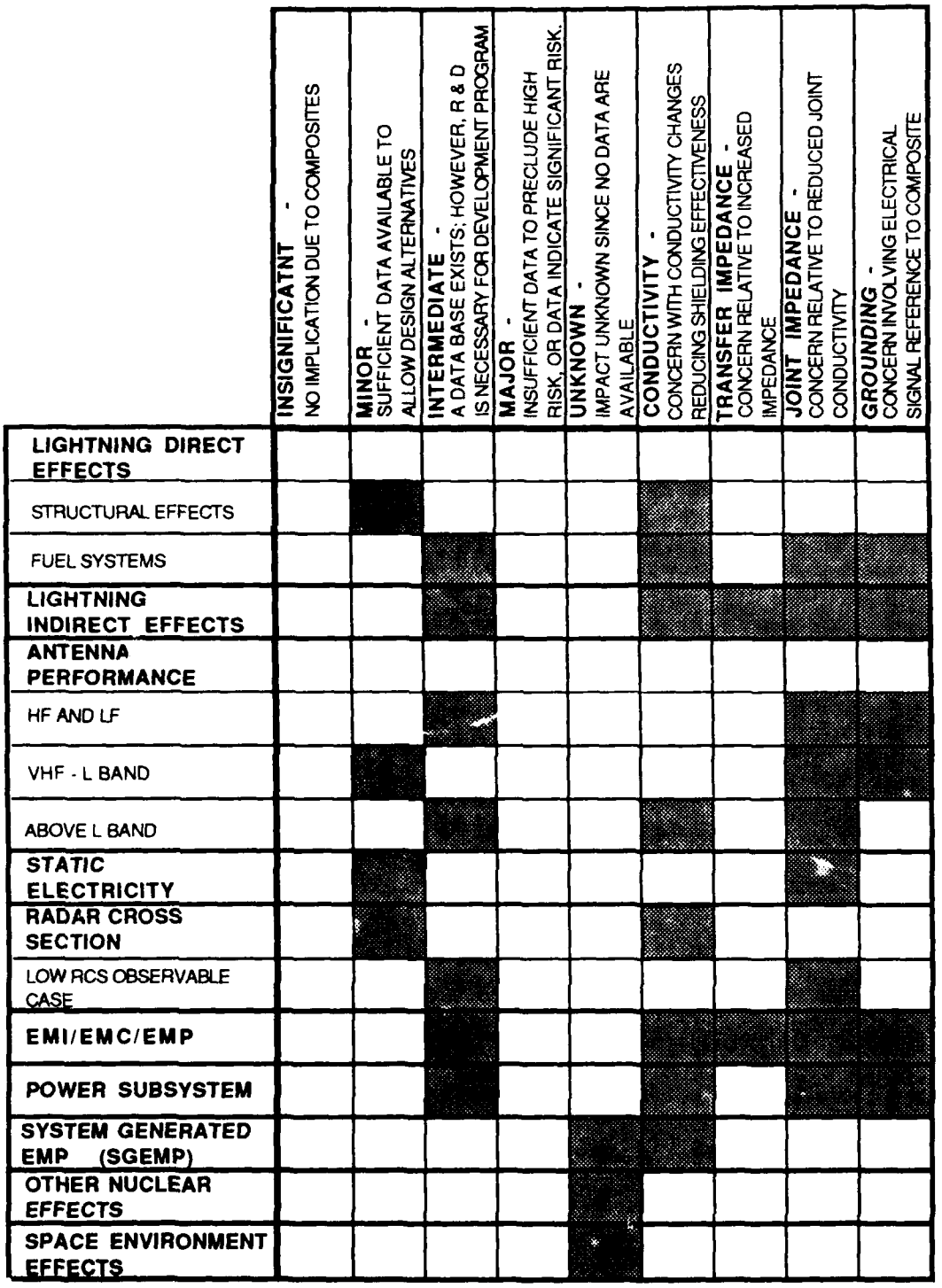

FIGURE 2. BONDING AND GROUNDING CONCERNS

Subsequently, a Tri-service, NASA and FAA working group was organized to consider these needs, providing program coordination, design guides and handbook development, information exchange, specifications and standards development or changes, and development of standard test methods for critical areas such as shielding.

RELATIVE SEVERITY OF AIRCRAFT EM ENVIRONMENTS.

Aircraft are exposed to a wide variety of EM environments from onboard and external sources including the following major items:

- The electrical power and electronics equipment often require that electric currents flow in the structure, if not by design, at least through equipment faults or short circuits.
- Lightning strikes to an aircraft result in large currents of short duration. These currents may flow in the structure and in any of the metallic plumbing, control cables, or wiring for the electrical/electronic systems.
- Antennas on the aircraft and nearby high energy RF sources may cause large RF currents in the structure.

The most severe EM environment is lightning. Direct strike lightning currents may be as high as 200 kA and the rate of rise may exceed 100 kA/usec. The effects of such currents will be subsequently discussed. Power system and electronic fault currents may reach a few thousand amperes (28 volts dc / 28 milliohms = 1000 A), while RF current density may reach a few tens of amperes per meter (10,000 volts/meter / 377 ohms = 26.5 A/M). The effects of these latter currents depend upon how much structure is in their path. Lightning and electric circuit faults act upon a small point of contact, hence could damage the structure at entry points. The RF currents are not likely to result in structural damage but could cause a functional disruption of the analog circuits and possibly of digital electronic circuits as well.

LIGHTNING ENVIRONMENT.

Interaction and Coupling to Aircraft. It is not possible to precisely quantify the lightning environment during any particular strike to an aircraft in flight. Lightning environments have varying intensity and duration because of the several different physical processes involved. During a storm, air convection currents cause charge centers to build-up within clouds. Because of mutual capacitance, the potential between these centers increases, and will eventually break down a portion of the air path between them and redistribute the charges. Once begun, the breakdown process proceeds in steps of the leader growth, shown in Figure 3, until a source of opposite charge, such as the ground or another cloud, is connected by the leader path and discharges the leader. The discharge path between charges then supports one or more high level return pulses, until the charges are neutralized. The number of pulses and the levels of current depend upon many factors including the storm intensity, the charge levels in the cloud before the leader path to ground is completed, and the height of the cloud base above ground. These factors are variable and more than an order of magnitude difference may occur between the currents of successive strikes.

It is generally accepted that the presence of an aircraft may trigger the leader discharge process between charge centers by disrupting the leader path. Recent flight experience by the FAA and AFWAL in-flight program using a CV580 to intercept lightning strikes indicates leader growth out of the wing of the test aircraft. When the aircraft is part of a leader not much current flows. The major effect occurs when the path is complete to the opposite charge center, and the return current passes through the aircraft. This leader growth happens in a short interval, the rate of growth being about 50 meters/microsecond. The seemingly long duration of a lightning strike is due to the many return strokes, i.e. restrikes that follow the same heated path, and lastly, the visual effect that persists for some time after the discharge is over.

A typical lightning "flash" consists of 20-200 current pulses over a one to two second interval. Each pulse may have somewhat different levels of current and waveform parameters. Because the aircraft is moving, the "flash" will sweep aft from an initial attachment point, all the while reattaching to spots along the line of flight aft from the original point of attachment. A portion of the current will enter the aircraft at several points along the path from the initial and swept attachment points. If the attachment is a trailing edge surface, then the current will hang on at this initial point and flow through there for the entire flash.

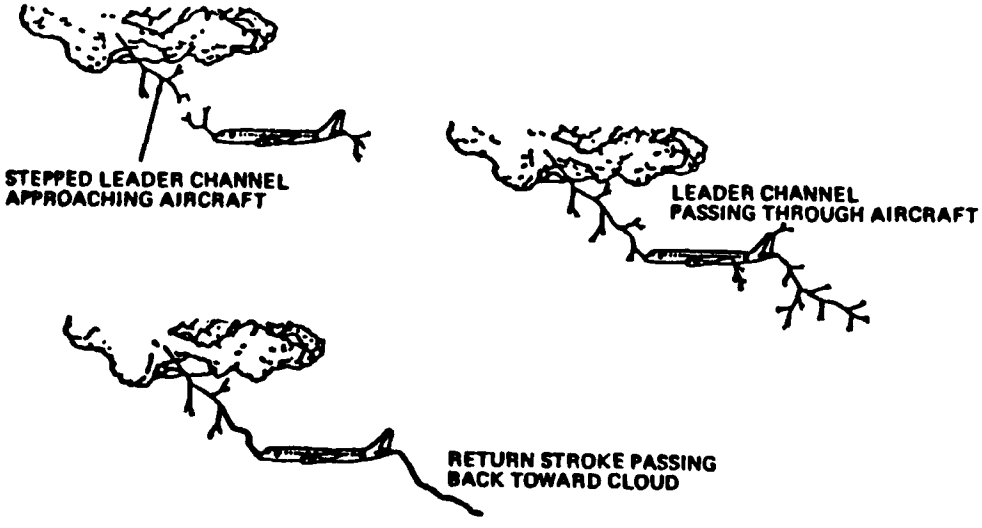

FIGURE 3. LIGHTNING FLASH STRIKING AN AIRCRAFT

Standard Aircraft Lightning Environment. Since different parts of an aircraft must tolerate different levels of current, a standard definition has evolved defining the levels of current applicable to different zones of the aircraft. The Society of Automotive Engineers (SAE) Committee, SAE-AE4L, has established generally accepted definitions of the possible strike zones as follows:

Zone 1A: Initial Attachment Point with low probability of flash hang on, such as a leading edge.

Zone 1B: Initial Attachment Point with high probability of flash hang on, such as a trailing edge.

Zone 2A: A swept stroke zone with a low probability of flash hang on, such as a wing midspan.

Zone 2B: A swept stroke zone with high probability of flash hang on, such as wing inboard trailing edge.

Zone 3: This zone includes the remainder of the vehicle that is not covered by Zone 1 and Zone 2. In Zone 3, there is a low probability of any attachment of the direct lightning flash arc. Zone 3 areas may carry large amounts of electric current, but only as a result of conduction between pairs of direct or swept stroke attachment points.

The location of strike zones is well established for current aircraft configurations, but if the configuration differs much from today's aircraft, locating the lightning strike zones may require careful interpretation of the particular geometry to determine the location and extent of the areas where lightning may attach, sweep, and hang-on.

The SAE-AE4L committee has also established the current levels to be expected in each of the strike zones to be used for test or certification purposes. An idealized representation of these defined current components for a complete flash is shown in Figure 4.

Structural Materials Effect on Strike Zones. An AF study by Grumman Aircraft Company investigated the strike attachment zones for an advanced fighter configuration. A scale model of the aircraft was used having replaceable panels for portions of the skin. The panels were made from aluminum, graphite epoxy, and kevlar. The study concluded that there is no essential difference between the strike zones for panels of graphite epoxy and aluminum. However, there is considerable difference for kevlar panels. Kevlar is a non-conductor, hence a lightning arc will jump over or along the surface rather than attach to kevlar.

Other studies have shown that the lightning arc will punch through kevlar to reach metal portions under kevlar skin panels. This is also reported to be the case for radomes used to cover nose-mounted radar equipment. Lightning will readily puncture a radome to reach metallic portions of an all-metal aircraft. These items are described in the report by Fisher and Plumer (Reference 4).

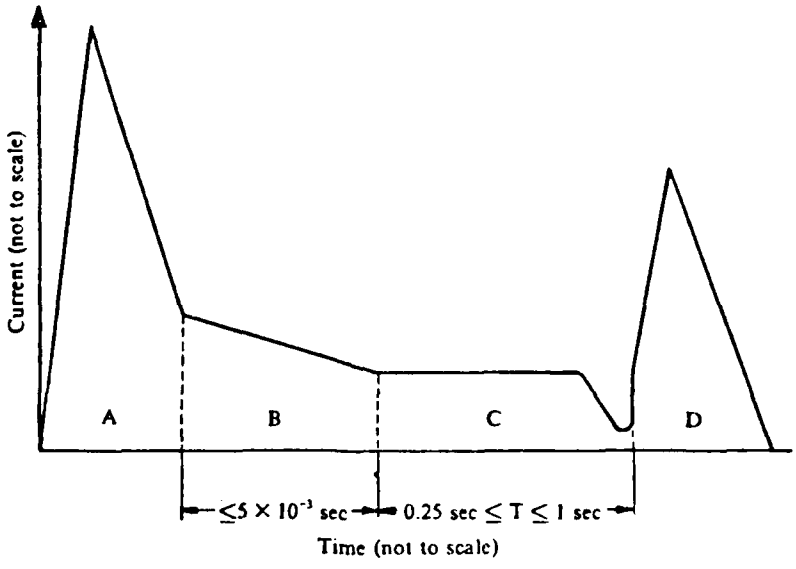

COMPONENT A (Initial Stroke)
Peak amplitude = 200kA ± 10%
Action integral = 2 x $10^6 A^2 \cdot s$ ± 20%
Time duration ≤ 500 μs

COMPONENT B (Intermediate Current)
Maximum charge transfer = 10 Coulombs
Average amplitude = 2kA ± 10%

COMPONENT C (Continuing Current)
Charge transfer = 200 Coulombs ± 20%
Amplitude = 200-800A

COMPONENT D (Restrike)
Peak amplitude = 100kA ± 10%
Action integral = 0.25 x $10^6 A^2 \cdot s$ ± 20%
Time duration ≤ 500 μs

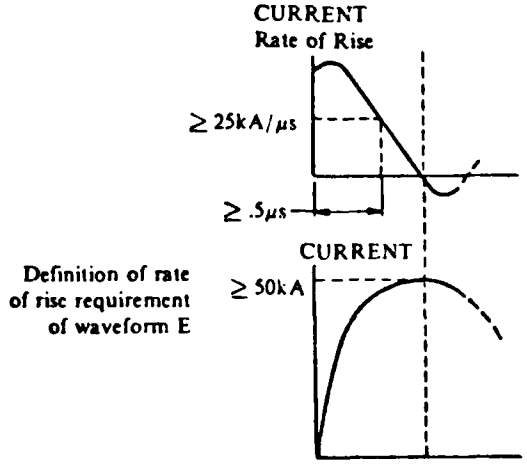

CURRENT WAVEFORM E
Peak amplitude ≥ 50kA
Rate of rise ≥ 25kA/μs
for at least 0.5μs

FIGURE 4. PRESENT SAE-4L RECOMMENDED LIGHTNING CURRENT TEST WAVEFORMS

LIGHTNING EFFECTS ON AIRCRAFT SYSTEMS.

Range of Lightning Effects. The range of possible effects from lightning strikes to aircraft in flight, shown in Figure 5, arises from two main factors:

- o direct effects -- physical damage from arcing and sparking and,
- o indirect effects -- disruption of the electronic/electrical systems from electrical transients in the wiring and structural elements.

Direct effects result from direct action of the lightning arc in the form of arcing and sparking on the aircraft, hence the term "direct effects." Evidence of this is seen as gross damage from the action of the arc on the materials. Protection against direct effects must come from the structure or protective diverters which prevent the currents from flowing into the sensitive areas. Damage may also occur from indirect effects that damage components or disrupt the software operations of electrical and electronic systems. Indirect effects are generally more subtle than direct effects. This is because the physical damage from indirect effects is not easily seen. Indirect effects are caused by the transient voltages and currents that are induced into the wiring as a result of the lightning arc and associated electromagnetic fields on the aircraft structure.

Indirect Effects Coupling Mechanisms. The mechanism for coupling of the external currents and EM fields into the wiring is by electric and magnetic induction and resistive drops. When lightning currents flow in the structure, electric and magnetic (EM) fields build up and change rapidly in accordance with the lightning current pulses. Some of these EM fields will leak into the internal portions of the aircraft through openings in the structure such as windows, radomes, access panels and doors. Electrical imperfections such as joints, gaps, and holes also allow the entry of some EM fields. In addition to the EM fields coupling, there may be resistive voltage drops in the structure as lightning currents flow. Currents may also flow inside the structure as a result of structural interconnections which can affect the internal EM environments.

Voltages are coupled into aircraft wiring in several ways. If part of a circuit connecting electronic equipment connects to structure, there will be a voltage difference between the wires and the structure. Voltages are also coupled between wires by electric and magnetic induction, even if the wires are not connected to structure. The effects of induction depend upon the time rates of change of the lightning currents and EM fields. Since the total structural voltage drops depend upon both the inductive and resistive terms, voltages in the wiring depend upon the lightning current time rate of change as well as the peak current values.

For an aircraft made of aluminum, the coupled voltages are rarely important except when the lightning current flows through joints and hinges. However, the resistance of advanced structural materials such as graphite epoxy and exotic aluminum alloys is many times that of aluminum. Voltages of a few tenths of a volt have no effect in an aluminum structure. Voltages that are larger by a factor of several hundred to a thousand times than those for aluminum because of the much lower conductivity of the composite materials can become very serious.

EFFECT	CAUSE	CRITICALITY
Flight Control Disruption	Low Tolerance to Electrical Transients Caused by Indirect Lightning or Static Electrification Effects. May Simultaneously Affect Parallel Redundant Systems.	Minor to Catastrophic
Fuel Tank Fire or Explosion	Fuel Vapor Ignition may be Caused by Static Electricity or Lightning Direct Effects on Structure. Fuel Gaging and Flow Management Electrical/ Electronics may Spark from Indirect Effects.	Minor to Catastrophic
Loss of Engine Power	Possible Direct Effects may be Caused by Acoustic Shock at Engine Inlet, or Loss may be Due to Indirect Effects or Electrical Transients on Engine Controls.	Minor to Catastrophic
Radome, Canopy, & Windshield Damage	Direct Effects of Lightning Strikes and Arc Discharge may be Caused by Static Electricity Buildup.	Minor to Catastrophic
Instrumentation Problems/ Communications, Navigation & Landing System Interference	Indirect Transient Effects may be Caused by Static Electricity Buildup and Nearby or Attached Lightning Strikes.	Minor to Catastrophic
Structural Damage	Direct Effects of Lightning Attachment to Aircraft may Damage Aircraft Structure.	Minor to Catastrophic
Physiological Effects on Crew	Flash Blindness & Distracting Electrical Shock may be caused by the Direct Effects of Nearby or Attached Lightning Strikes.	Minor to Catastrophic
Inadvertent Deployment of Landing Gear or Control Surfaces	Premature Activation may be Caused by Indirect Effects of Lightning or Static Electricity Buildup in Electrical / Electronic Systems.	Serious to Catastrophic

FIGURE 5. RANGE OF POSSIBLE EFFECTS FROM LIGHTNING STRIKES

Direct Effects on Non-Metallic Structures. The most important direct effect of lightning strikes is the possible arcing & sparking in fuel areas. Other important direct effects include deeper pitting and burning than occurs in aluminum structural materials of the same strength. Also fastening and joining methods require more attention and designs are now becoming available to provide adequate protection against lightning strikes.

For reasons discussed in later subsections, direct effects protection design requires more test and analysis for composite materials than for metallic materials. For example, it is usually assumed, in the design of lightning protection, that if an electrically conductive fastener is located in an attachment zone having a high probability of hang-on, lightning will attach to the fastener. Because of the currents in the strike zone definitions, the direct attachment to a fastener in a zone 1A, 1B, or 2B represents a severe worst case for any lightning strike. Although this is not overly severe in aluminum structures, it is presently not possible to develop a fastener to join advanced composite materials capable of carrying the full lightning current without seriously weakening the fastener. Current composite aircraft designs depend upon not having fasteners in critical parts of zone 1 and 2. Where fasteners are used, a repair procedure may be necessary for lightning strike damage.

Painted metal surfaces have longer hang-on times for swept strokes than do unpainted metal surfaces. These longer dwell times will cause deeper burning and additional metal is required for painted metal skins on wet wing aircraft.

Composite materials have various resin binders that burn and affect the dwell time for swept strokes. Hence the thickness of composite materials required for structural integrity protection against lightning strikes will depend upon the materials makeup as well as the fibers. It is expected that different materials of the same physical strength will behave differently when struck by lightning.

The electrical properties of joints and fasteners are as important as the properties of the underlying structural material in determining the strength of members following lightning strikes. Although it is possible to make a perfect joint - one that doesn't add to the resistance of the basic materials that are being joined - they usually do add to the resistance. The concentration of current flow around fasteners usually causes local heating that weakens the joint before the bulk material being joined fails from over heating. These failures are usually evidenced by sparks that shower from the fastener area.

Indirect Effects On Non-Metallic Structures. The most important adverse feature of graphite and metal matrix materials is their lower conductivity. The conductivity factor, compared with aluminum, is 10 times less for metal matrix and 1000 times less for graphite epoxy. Lower conductivity means higher voltage drops in these structures than for a metal structure. Thus the voltage drop in a length of structure will be increased for the same level of lightning current. Because of the higher voltage drop, higher levels of currents will flow in any metallic paths such as plumbing and wiring inside an aircraft structure made from non-metallic materials. Additionally, any external electromagnetic fields will be attenuated less by a composite structure. For direct and nearby strikes, the internal EM

fields will be at higher levels than for an aluminum aircraft. The exact difference in internal EM fields depends on the number of joints and openings, thickness of material, frequency range of the external EM fields, and the shape of the structure. The Atmospheric Electricity Hazards Protection (AEHP) program studies on an advanced composite (gr/ep) structure F-16 fuselage showed that the shielding was 15 dB for lightning pulses. It is estimated that a similar aluminium structure would have provided 30-40 dB of shielding, the limitation being primarily due to the number and size of openings.

In structures made from non-conductors, there is no EM shielding. This is also true for materials having very few conducting wires embedded into a non-conducting material such as Thorstrand kevlar. Although these materials can provide suitable protection against direct effects, there will be little or no improvement against indirect effects. This is because the magnetic shielding effectiveness of low loss factor metals, such as aluminum, is primarily due to currents flowing in the material that generate EM fields which tend to cancel the incident fields. Electric field shielding is primarily due to an equipotential plane established by high conductivity metals. There are too few wires and too little metal in a material like Thorstrand to provide an effective shield against EM fields from nearby lightning or RF sources, such as airport radio and radar transmitters.

STRUCTURAL GROUNDING AND BONDING.

Present 2.5 Milliohm Requirement. The present specification MIL-B-5087 for military systems calls for a 2.5 milliohm resistance between units of electronic equipment. This specification is not difficult to meet for aluminum structures. The resistance requirement was established early on by the Electromagnetic Compatibility (EMC) community to assure that potential interference sources in different equipment would be isolated from sensitive electronics. The basis for the number chosen was one of engineering judgement. If the resistance was zero, there would be no interference. The value of a few milliohms is not too stringent a requirement for aluminum structures where subelements (fasteners, racks, etc.) typically have tenths of a milliohm resistance.

Grounding and bonding specifications have been evaluated over the years through in-service experience and laboratory testing in equipment qualification. For the most part, aluminum and titanium alloys present no major difficulties in meeting the 2.5 milliohm specification. Maintaining adequate conductivity throughout an airframe has been a problem only when good contact between mating parts could not be maintained. Breaks in conduction paths are necessary at doors, hinges and control surfaces; control of corrosion often requires a non-conductive coating on a part. Where interruptions in the grounding path occur, bonding requirements are met by reestablishing the conduction path using a metal jumper or strap.

Although the present specification provides good in-service experience, there is no general factor or body of experience that indicates the value of 2.5 milliohm could not be raised. It is particularly convenient to use the 2.5 milliohm value for assessment of system protection against lightning, for if 200,000 amp peak value current pulse flows in a 2.5 milliohm resistor then the maximum voltage drop will be 500 volts. If every bond has less than 2.5 milliohm resistance, then no end-to-end validation testing is necessary providing each unit of equipment will withstand 500 volts.

Requirements for Grounding and Bonding. Requirements for direct effects protection require that the grounding and bonding system be spark free in fuel areas, and that load bearing elements are not seriously degraded upon experiencing a lightning strike. Meeting these requirements requires an experimental approach.

Requirements for indirect effects protection of electrical/electronic systems against lightning strikes depend upon the meeting of operational requirements on the equipment. The need for adequate grounding and bonding is well established by operational experience. For example, aircraft having poor grounding and bonding (i.e., poor or no electrical conduction throughout the structure and wiring) may be subject to operational hazards varying from major to minor. When different parts of the aircraft and wiring are not electrically connected, differences in potential can build up between them. Since the ultimate breakdown potential of air reduces with altitude, corona or sparks may occur. Furthermore, fuses or circuit breakers to protect against shorts in equipment and wiring may not open properly. These factors lead to the following:

- o Fuel explosion hazards from sparking in fuel gauges and wiring.
- o Static discharges that may rupture windows (dielectric).
- o Personnel electric shock hazards.
- o Electronic equipment damage - burn out.
- o Electrical/electronic systems malfunctions.
- o Excessive radio noise when communicating with airport or other aircraft.

The electrical function of a bonding and grounding system for protection of electronic and electrical equipment is to provide a low impedance ground path for current flow. Table 1 indicates the current levels that may be expected.

The path impedance should be low enough that these interference sources will not produce a high voltage value that can disrupt equipment functions. Electrical/electronic equipment can be made to tolerate voltage differences between units of a few volts. Typical values for equipment tolerance against transients are shown in Table 2.

Tolerable levels of ground impedance, based upon the Tables 1 and 2 values are shown in Table 3. These data indicate that the range of acceptable ground impedance values depends upon the source of interference and the degree of protection built into the installation and equipment. Equipment containing large scale integrated circuits can be designed and built to withstand 600 volt potential differences. This level of protection requires balanced circuits, high impedance input networks, and twisted pair wiring. More typical circuitry can withstand 10 volts between units by using balanced circuits. Single ended digital circuits can only tolerate a few volts between units for Transistor-Transistor Logic (TTL) circuits that operate with 5 volt logic levels.

TABLE 1

GROUND SYSTEM CURRENTS FROM A VARIETY OF EM SOURCES

CURRENT SOURCE	RANGE OF CURRENT
1. Lightning currents, broad band pulses.	20 KA to 200 kA
2. Power systems fault currents, continuous wave 400 Hz.	100 A to 1000 A
3. RF current returns from on board transmitters and transponders, continuous wave HF, VHF, UHF, and microwave.	1 A to 10 A
4. Currents from nearby sources of RF energy such as radar and radio transmitters, continuous wave HF, VHF, UHF, and microwave.	1 A to 10 A
5. Power currents resulting from relays, strobe lights, and other high pulse currents devices.	5 A to 50 A
6. Digital and analog signals between units of equipment, CW and Puises 100 Hz to 10 MHz.	10 ma to 5 A

TABLE 2

TYPICAL INTERFERENCE TOLERA[illegible] TWEEN UNITS OF ELECTRONIC EQUIPMENT

1. Lightning Pulses (a)	600 volts
2. Power System Faults (b)	10 volt
3. Continuous Waves HF Frequencies	50 volts
4. Continuous Waves VHF Frequencies	100 volts
5. Continuous waves UHF Frequencies	100 volts
6. Tracking Radar (Sweep Frequency)	10 volts

NOTES: a. Specially protected against lightning by balanced signals, high impedance, and twisted pair circuits.
b. Circuits unprotected except balanced signals, twisted pair wiring.

TABLE 3

TOLERABLE LEVELS FOR GROUND IMPEDANCE IMPLIED BY TABLE 1 AND TABLE 2 VALUES

1. Lightning Pulses	3 to 30 milliohm
2. Power System Faults 400 Hz	10 to 100 milliohm
3. Continuous Waves HF	5 to 50 ohms
4. Continuous Waves VHF	10 to 100 ohms
5. Continuous Waves UHF	10 to 100 ohms
6. Tracking radar (Sweep Frequency)	0.1 to 1 ohm
7. Power Currents From Onboard Pulsed Current Devices	20 to 200 milliohm
8. Digital and Analog Signals	0.2 to 100 ohms

SECTION II - TEST METHODS EVALUATION

APPROACH.

The objective of this task is to evaluate the existing test methods for determining bonding and grounding parameters for metal, metal honeycomb, and advanced composite aircraft structures.

The approach involved the following activities described as follows:

1. Identify the test methods for determining electrical characteristics of structural elements and assemblies appropriate for lightning, static electrification, and RF environments, specifically those for:

   a. bulk material properties
   b. coating properties
   c. joint properties
   d. bonding properties
   e. grounding properties

2. Evaluate the methods for applicability to the bonding and grounding tests needed to characterize advanced technology aircraft structural materials. This evaluation included the following factors:

   a. Accuracy of the data achievable by the method.
   b. Accuracy of extrapolating the measurements to lightning threat environments.
   c. Do the test methods yield basic parameters that can be extrapolated to full scale structures and the localized threat environments?
   d. Do the test methods yield data on threshold current and breakdown voltage?
   e. Can the test data be used with the localized threat environments to establish a margin of safety against sparking, indirect effects transients or RF current return from antennas?

There is a large base of research and test data to draw upon for this task. Numerous technical conferences have been held on the topic of bonding and grounding, such as, the ones identified in Appendix A (References 1,8-10). These documents and the more specialized research reports on composite structures (References 19, 21, 22, 23 and 26) provided the bulk of the needed data. The remaining information presented is from technical notes compiled by the principal investigators and from their knowledge of EMI/lightning test technology.

There are many examples that could be quoted from the Appendix A references where the bonding and grounding systems and data are compatible. The documentation from the AEHP program, such as Reference 27, is also available for this program. Two available reports have been chosen as most useful. A recent NASA research report by A. Plumer (Reference 19) contains the most complete description of the test samples, configurations of subelements and a complete wing structure as well. The NASA data is the best available for these studies without additional extensive testing and structural test bed development -- much beyond the scope of this report. The

second source of data is documented in an older NASC research report by R.Force, et al (Reference 22); this report contains considerable data on small samples of composite materials including joints, bonding and grounding. These two documents were complete enough that the test setup, structural samples, and data are easy to correlate so that additional testing was not needed.

The NASA research (Reference 19) provides a complete link from the external structure to subelements and to the linear and nonlinear tests on the subelements. This work was intended to provide design guidance for general aviation aircraft. Two full scale aircraft were used as test beds -- a bonded aluminum structure and a graphite epoxy structure. Extensive tests were done in support of the design and results are reported in considerable detail. The subelement samples tested, described in Table 4, cover the full range of bonded metal and graphite structures. Figure 6 is presented to show the subelement definition. Full scale lightning simulation tests were also performed on the wings of the two aircraft. These tests allow correlation of the external environments to the subelements; the test configurations are shown in Figure 7.

Prior NASC research (Reference 22) also has important data to contribute. The research was directed to developing basic data for assessment of the electromagnetic problems that would be encountered in applying composites to aircraft. Small samples were fabricated for joints and panels of graphite epoxy. The samples were tested for electrical and mechanical properties, including lightning, static electrification, power faults, and EM shielding effectiveness. This data is very useful for power and grounding considerations.

TEST REQUIREMENTS.

The requirements for grounding and bonding test data govern the selection of screening test candidates. Data is required to determine the allowable levels of current that samples can withstand without arcing and sparking. Data is also required on the current distribution in a complete vehicle if it can not be assured that the entire current may safely flow in a single structural element (joint, bond, or basic structural skin).

The approach to assessing a design for lightning protection requires a comparison of the lightning current with the maximum allowable EM strength (current or voltage), and is shown in Figure 8. This figure indicates how the vehicle is divided into portions or coupons, and then a comparison is made between the allowable stress on the portions of the vehicle (coupons) and the expected stress on the locations corresponding to the coupons. The expected stress is determined from tests and analysis of the distribution of severe lightning currents on the full vehicle. Allowables for the coupons are determined from laboratory tests and analysis using lightning current simulators.

Grounding and bonding tests should be designed so that accurate data may be obtained by different investigators using the method, drawing the same conclusions about safety of the design when subjected to lightning currents.

A recommended breakdown of the test articles into specific portions of an aircraft is in Table 5.

TABLE 4

SUBELEMENT SPECIMENS TESTED BY NASA (REFERENCE 19)

Adhesively Bonded Aluminum: Bonded aluminum lap joint specimens: - with varied adhesives - with varied bond line thicknesses Bonded aluminum lap joint specimens: - with one rivet Bonded aluminum fuel line brackets Bonded aluminum honeycomb panels
Hardware Interfaces With Metals: Access doors riveted, fastened, or bonded and fastened
Adhesively Bonded gr/ep: Bonded gr/ep lap joint specimens: - with varied adhesives - with varied bond line thicknesses Bonded gr/ep lap joint specimens: - with one rivet Bonded gr/ep stiffeners
Metal-to-gr/ep Interfaces: Rivets in gr/ep laminates: - covered with fuel tank sealant - uncovered Access door dome nuts in gr/ep laminates Fuel line feed-through elbows in gr/ep laminates

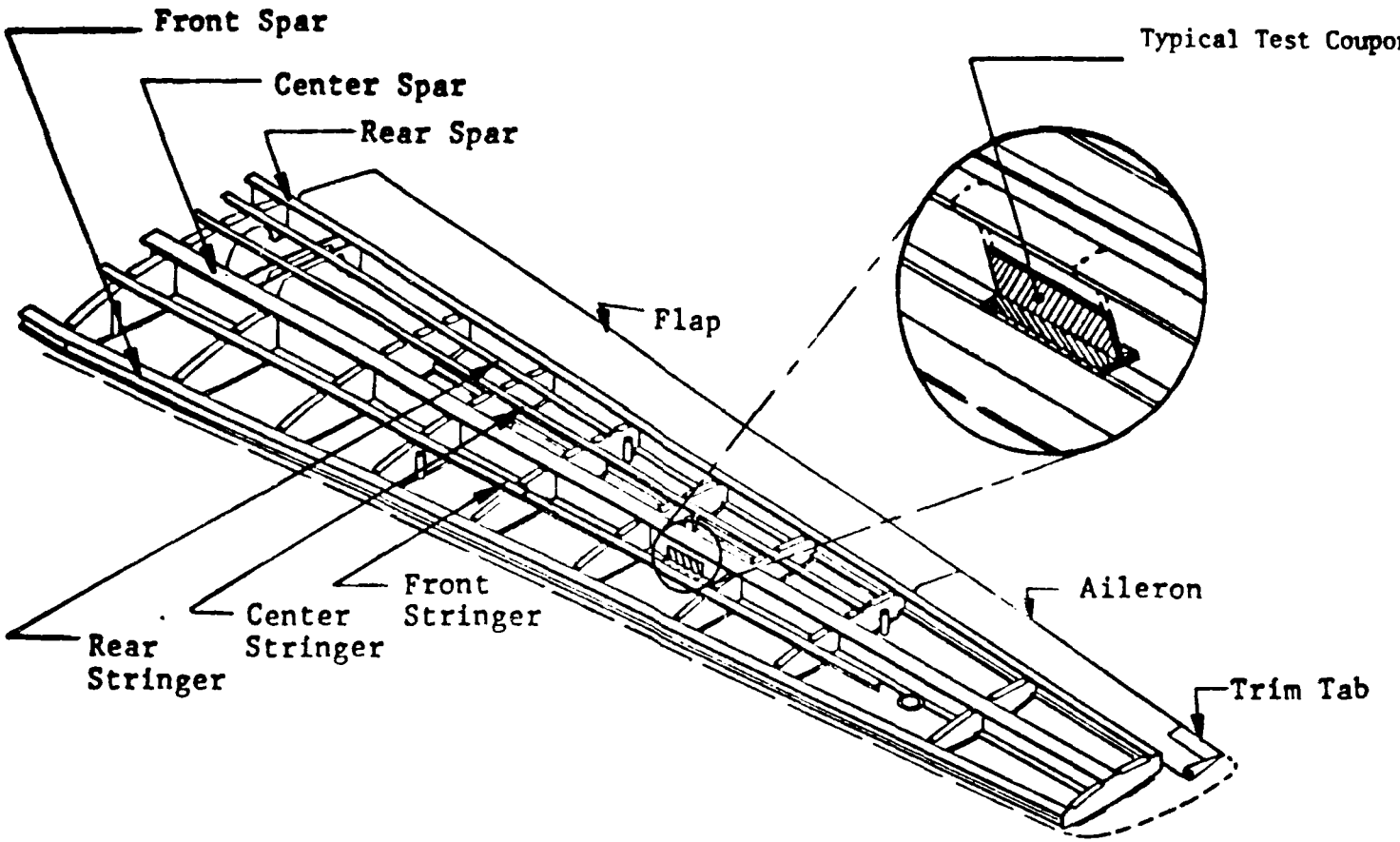

FIGURE 6. GR/EP WING INTERIOR VIEW

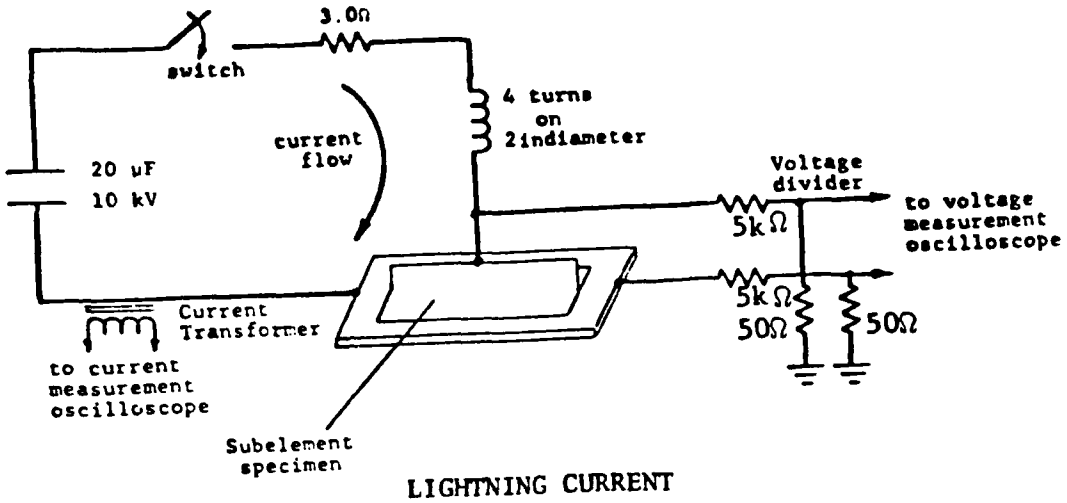

LIGHTNING CURRENT

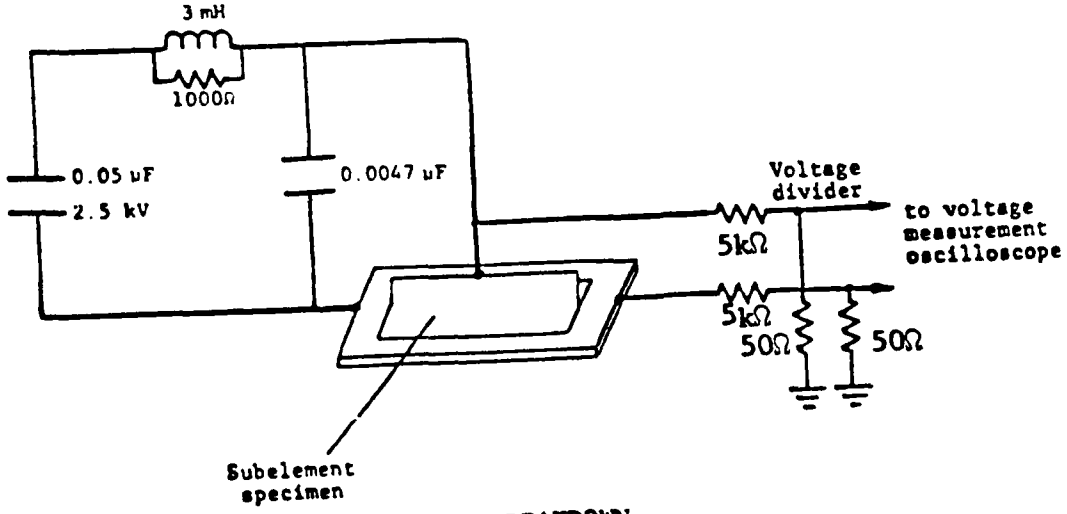

VOLTAGE BREAKDOWN

FIGURE 7. TEST CONFIGURATIONS

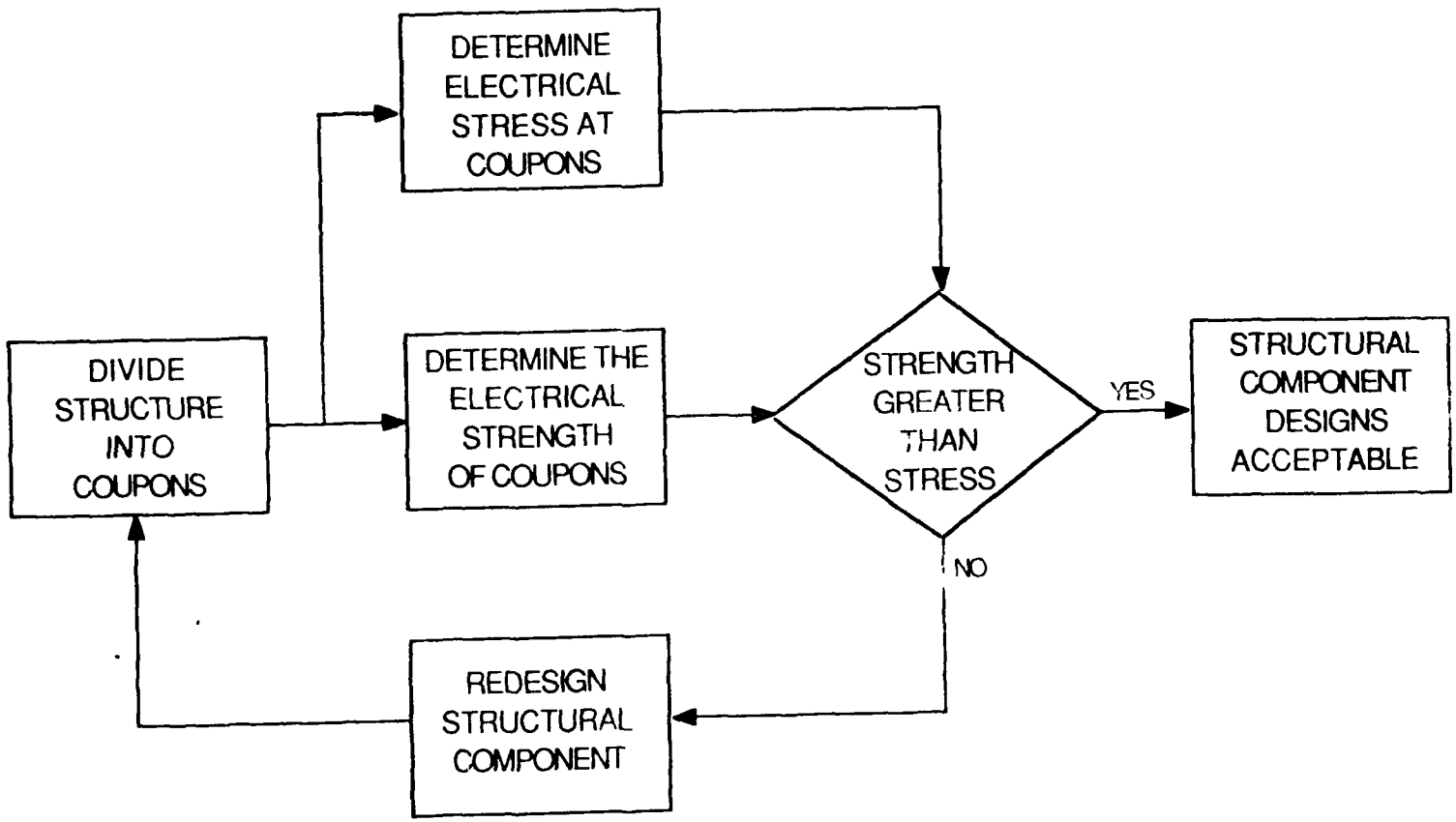

FIGURE 8. DESIGN FLOW DIAGRAM

TABLE 5

TEST ARTICLE RECOMMENDATIONS

TEST ARTICLE	DIRECT EFFECTS	INDIRECT EFFECTS
Complete vehicle	Not Required May be performed on small vehicles rather than coupons or subassemblies.	Test required to validate key assumptions on EM coupling
Subassemblies	May be substituted for coupon tests	May be substituted for full vehicle to validate assumptions on EM coupling
Subelements coupons	Recommended for determining allowable currents voltages	Needed to determine parameters of materials

TEST METHODS REVIEW.

A summary of the existing test methods identified during the review of available literature on grounding and bonding test methods, is shown in Figure 9, where the range of applicability is indicated for various structural sample sizes from small flat sections through cylindrical sections, structural elements, subassemblies and full vehicles. Two different test types are described:

a. tests for determining the basic electrical properties of bulk materials, bonds and joints;
b. tests for breakdown effects such as voltage breakdown and sparking thresholds.

Bulk Properties. Bulk electrical properties of materials (resistivity or conductivity) are measured directly using a small sample of the material. These measurements can be made at dc or a low ac frequency (1000 Hz). Several instruments are available for both ranges of frequency. Measurements of bulk electrical parameters of graphite and other conducting fibers embedded in any cured resin material are complicated by a directional conduction in the gr/ep composite. This is due to poor or zero conduction in the resin materials. Common epoxy has 1/100,000,000 the conductivity of graphite. Hence the conduction of the composite material is entirely due to the graphite fibers. This results in a unidirectional conduction along the graphite fibers in

TEST \ PURPOSE	BULK PROPERTY	JOINTS	BONDS	GROUNDING	COATINGS
Four Point Resistance Conductivity Flat Samples	X			X	X
TEM Cell-Flat Samples	X			X	X
Coaxial Cylinder Samples	X	X	X		X
Quadrax-Flat Samples	X	X	X	X	
Cylinder-Cir. Joints	X	X	X	X	X
Sparking Thresholds Subelements		X	X		
Breakdown Voltage Subelements		X	X		
Structure-Resistance		X	X	X	
RF Current Return Impedance				X	
Antenna Bonding Resistance			X		
Static Charge Discharge	X				X
High E Field Corona					X
Full Vehicle Coaxial	X	X	X	X	X
Full Vehicle Shock Excited	X	X	X	X	X

FIGURE 9. EXISTING TEST METHODS COVER A WIDE RANGE OF SAMPLES AND TECHNIQUES

individual layers. The fibers normally conduct along the direction of the material lay-up and poorly (if at all) across the fibers. The extent of the anisotropic conductivity depends upon the pressure applied during the cure process. The differences in conductivity are very great for unidirectional fibers as found in mats of material. This was particularly important for early users of these materials where the mats were the first available form. Fortunately, the structural properties are similarly affected by the directional lay-up of the fibers, being weak across the fibers, and single lays are rarely used, if at all. This is not as severe a problem at present because most materials are now available in a woven cloth where there is contact between the two directions of the fibers. For a single layer of cloth material, the resistance is the same at a zero and 90 degree orientation, and 71% of that value at 45 degrees. Commonly four plies are used at two different orientations, 45 degrees apart so that conduction is nearly the same for any edge-to-edge measurement in a sample of structure.

The following three bulk parameter measurement methods are reported in the literature and are briefly described below:

a. Surface resistance.
b. Volume resistance.
c. Edge-to-edge resistance.

The apparatus for surface resistivity measurements is shown in Figure 10. This measurement is useful for coatings and to determine if the fibers are coated with epoxy at the material surface. Pressure is applied to the fixture to make a positive contact with the material sample. Surface resistance measurements, reported in Reference 22, depend upon the applied pressure.

TABLE 6

SURFACE RESISTANCE

Ply Thickness	Resistance, Milliohm			
	Longitudinal Fiber Orientation		Transverse Fiber Orientation	
	With Epoxy Layer	Without Epoxy Layer	With Epoxy Layer	Without Epoxy Layer
4	128	73	205	150
16	225	135	337	225
32	220	290	570	420

Sample measurments are shown in Figure 11. An extrapolation is used to infer the value at zero pressure. Table 6 summarizes the surface resistance data for different sample thicknesses. It may be noted from the Table 6 data that the surface resistance increases with sample thickness, counter to what may be expected. This trend in resistivity is due to the additional current paths available by penetration into the materials deeper layers. This measurement technique provides information on how well the different layers make contact. Thus the value of resistance depends upon how well current flows in to the

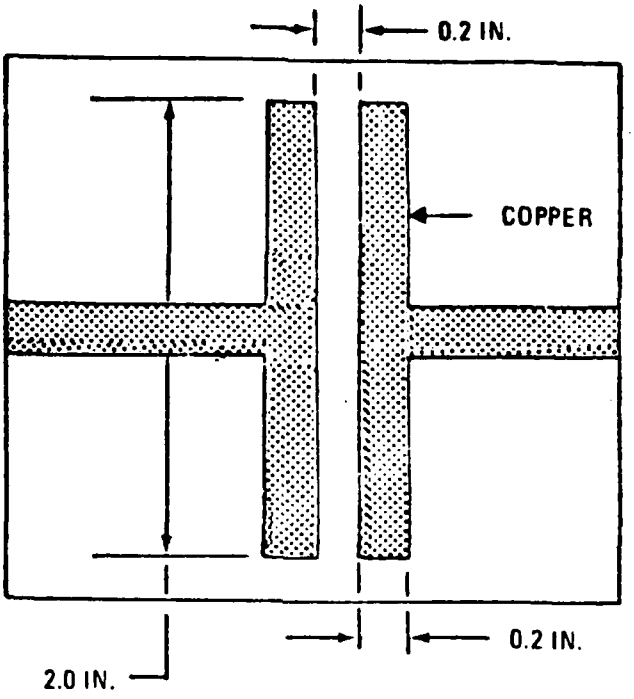

a. SURFACE PROBE DIMENSIONS

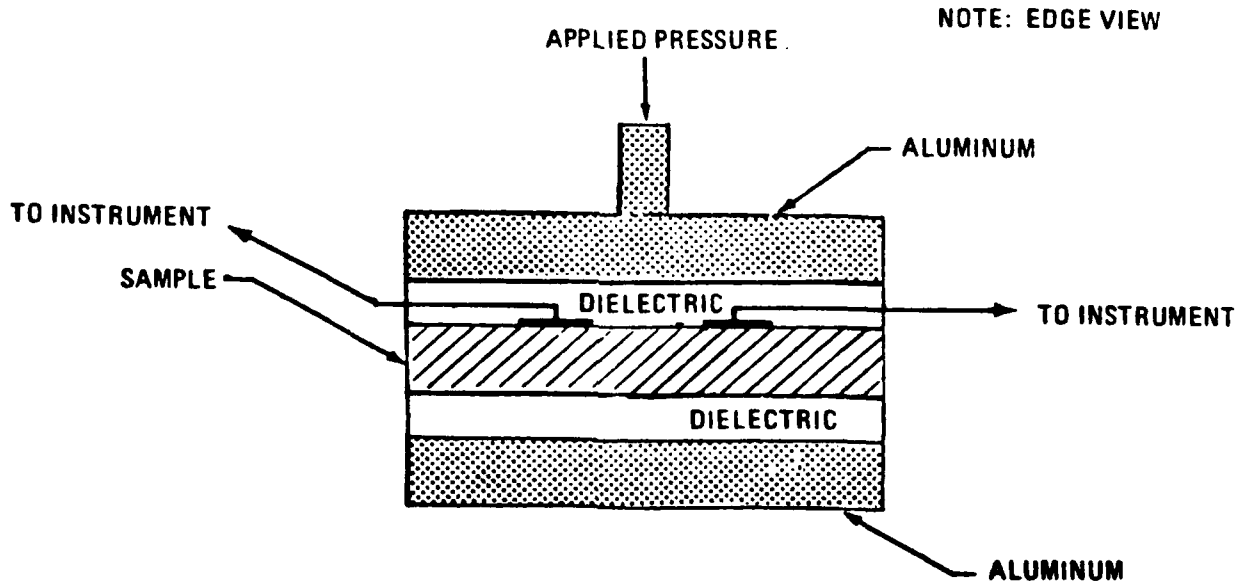

b. EDGE VIEW OF PROBE

FIGURE 10. EXPERIMENTAL APPARATUS FOR SURFACE RESISTIVITY MEASUREMENT

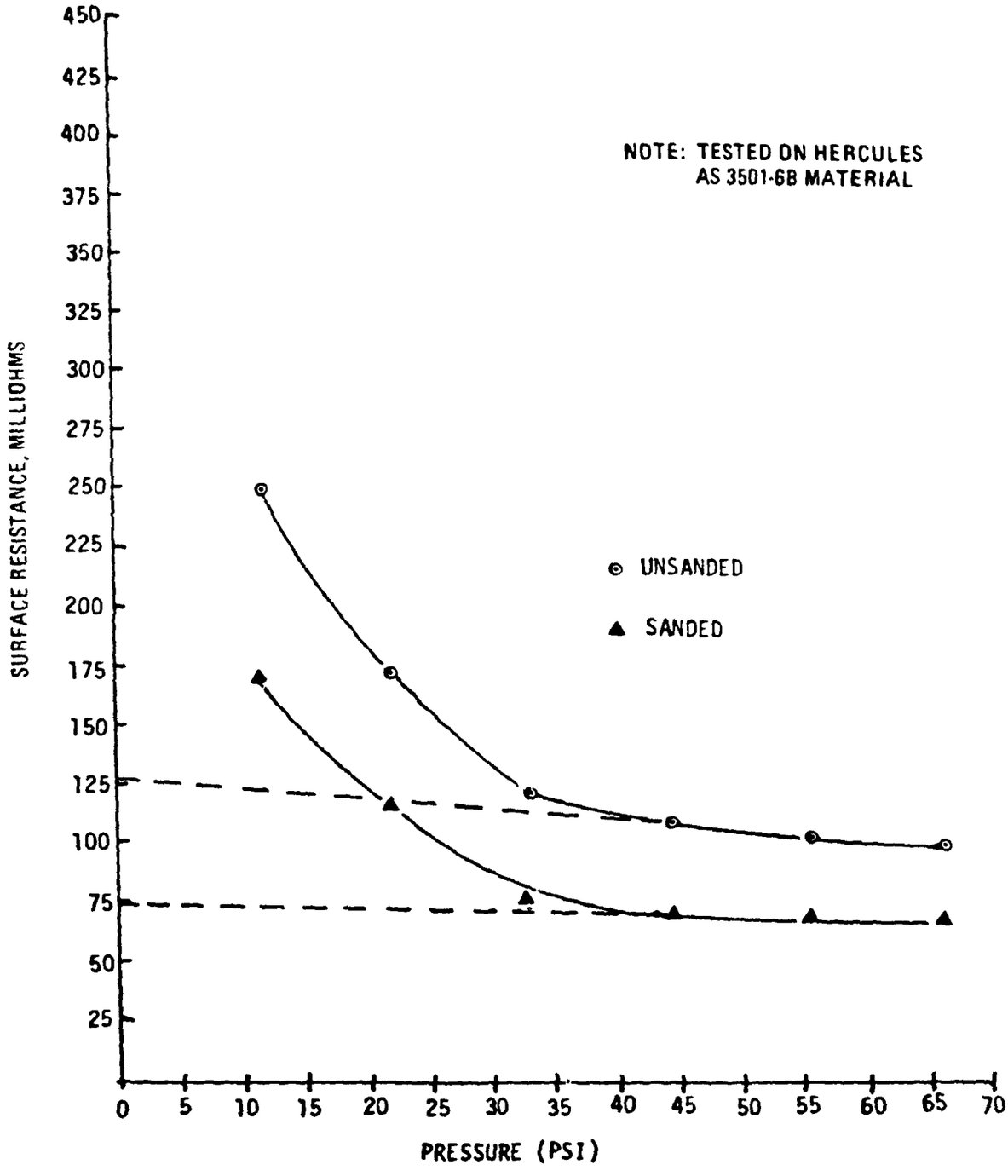

FIGURE 11. FOUR CROSS PLY, LONGITUDINAL FIBER ORIENTATION WITH AND WITHOUT EPOXY LAYER

material from the surface layer. Although this may be an important test for manufacturing repeatability, this method is not recommended for use to determine resistance for the lightning current paths for two reasons: the lightning current must flow through all the layers of material, and the current is so large that provisions are needed to distribute the current into the material at a point of contact. For lightning currents, the main issue is the burning and extent of the damaged area; this information cannot be determined by a resistance measurement. Lightning damage at an attachment or penetration point depends upon internal pressures that build up from the rate of burning and depth of penetration of the current into the materials.

TABLE 7

VOLUME RESISTANCE AND RESISTIVITY

PLY THICKNESS	MEASURED RESISTANCE MILLIOHM	COMPUTED RESISTIVITY MILLIOHM-M
4	64	82.0
16	160	51.2
32	287	45.9

Volume resistance measurements reported in the literature (Reference 22) used the setup shown in Figure 12. Volume resistance data, shown in Table 7, indicates an increase with sample thickness, as may be expected since

$$R = \rho \, l/A,$$

where ρ is the resistivity of the material, l is the length and A is the cross sectional area of the current flow which is proportional to thickness. However, the resistivity value computed from the measurements decreased with increasing sample thickness. A volume resistance measurement may have some usefulness in a manufacturing quality assurance program because it depends upon the degree of contact between successive layers of the fiber materials. Measurements of bulk resistivity using this method are unreliable; sample thickness should not be a parameter in the resistance value. This method is likewise not recommended for measuring resistance of lightning current paths since the lightning currents should not be allowed to flow from face to face of a composite material without some provisions to guide the current into the fibers by using fasteners or metallic conductors.

Measurements of resistance from edge to edge on a square sample may be used to determine reliable values of resistivity for different sample thicknesses. Measurements in the literature (Reference 22) used samples having a symmetrical lay-up (0,+45,-45, and 90 degree) in the fiber orientation. The edge was trimmed and electrical contact made between the fibers and a layer of copper deposited by an electrodeless plating technique. Silver paint has also been used by others. The measured data are consistent with a simple resistor model whereby resistivity may be calculated from the

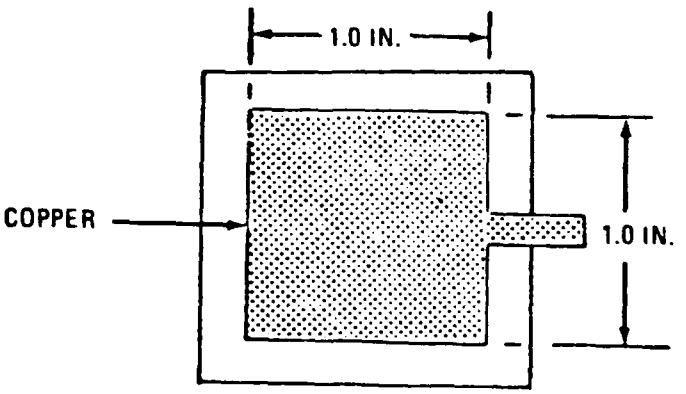

a. VOLUME PROBE

NOTE: EDGE VIEW

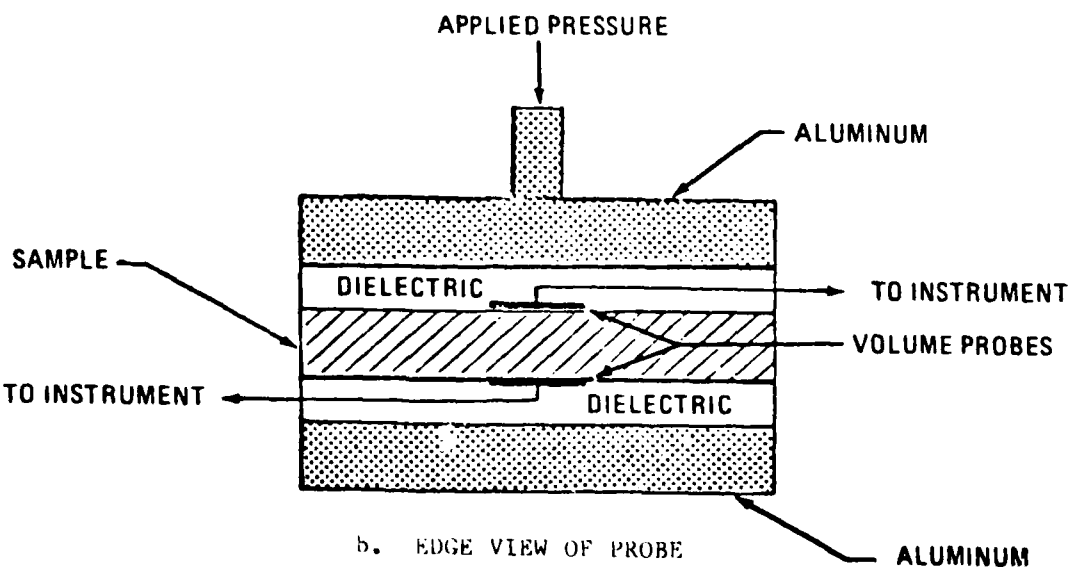

b. EDGE VIEW OF PROBE

FIGURE 12. EXPERIMENTAL APPARATUS FOR VOLUME RESISTIVITY MEASUREMENT

measured resistance using

$$\rho = RA/l$$

A set of data from Reference 22 is shown in Table 8. The values were repeatable within 6 milliohms. This measurement method is recommended for determining bulk material properties of epoxy fiber materials where it is necessary to have repeatable data on different thickness of material. The underlying accuracy of this method is due to the conduction being confined to the normal current carrying direction of the fiber layers rather than across the layers.

Table 8

Graphite/Epoxy Edge-To-Edge Resistance Data

Ply Thickness	Resistance, milliohms measured edge-to edge	Resistivity, computed edge-to-edge microohm-m
16	162	64.3
32	89	65.7

It should be noted that the value of resistivity obtained by the edge to edge method is valid for other means of initiating current into the materials, as for example an incident EM wave, providing the frequency of the incident wave is less than the skin depth frequency for the material which is given by:

$$f = \frac{1}{\pi \sigma \mu t^2}$$

where t is the material thickness, σ is its conductivity, and μ is its permeability. The above condition assures that, for frequencies below the skin depth frequency, the current penetrates uniformly into all the layers of the material. For four ply graphite epoxy material this condition is met for frequencies up to 10's of Megahertz.

Electrical Bonding and Grounding. Electrical connections to the structure are necessary to assure personnel safety against electric shock. If an equipment enclosure is ungrounded and a fault occurs in the power distribution system, hazardous voltages then will build up between the structure and electrical equipment. By grounding the equipment, any faults between the power and chassis will cause a short circuit on the power system, rather than allow the build up of hazardous voltages. Tests on the bonding connections from power returns to the structure use small samples and a configuration of fasteners. Measurements are made showing the

temperature rise and voltage drop in the fastener for different fault currents.

Results presented in Figure 13 (from Reference 22) show representative data from tests on a graphite epoxy panel 18 x 18 inches with two different fasteners. The results of these tests concluded that the minimum bond resistance was 0.01 ohms for a single connection and 0.0048 ohms for three bonds in parallel. Neither of these bonds complied with the requirements of MIL-B-5087B for bonds in explosion hazard areas. It is unlikely that the 2.5 milliohm specification value can be met for composite material structures. However, the intent of the MIL-B-5087 specification, i.e. to control possible ignition sources in an explosion hazard area, must be maintained.

At sufficiently high currents, sparking will occur at connections between metal and graphite epoxy composite materials. Tests are recommended to establish the breakdown limits for each type of bonding connection where high currents may flow. These tests are subsequently described under the heading of joint breakdown tests.

Joint Resistance Characteristics. Joints in the materials composing an air vehicle create additional resistance over that of the basic materials in the lay-up. In many instances the resistance of joints and fasteners will limit the amount of lightning current that a portion of structure can handle. Suitable values for joint resistance may be obtained using low frequency (dc to a few kilohertz) methods and conventional electrical measurement equipment. Low frequency measurements will provide resistance (R) and inductance (L) values for the joint applicable to power frequency and lightning currents. Samples may be constructed from a sample of the materials to be joined and one fastener. The sample width should equal the fastener spacing, and the length two to three times the width. The test sample should have the fastener placed in the same position from the edge as in the application. The geometry of the second (joined) panel should be the same size as the first. Panels joined by a backing plate should also be tested in a symmetric manner with the backing plate full width and the joined pieces the same size. The Analytical Models section of this report discusses results of tests and analyses on samples having these configurations.

Basic electrical resistance properties of joints may also be measured over a much wider frequency range (kilohertz to 100 Mhz). Such wide band measurements use idealized flat or cylindrical samples in an EM test cell, such as shown in Figure 14 for joint characterization (from Reference 22). Although beyond the scope of a grounding and bonding study, it should be noted that data from such measurements can be used to determine the electrical shielding effectiveness of complete portions and entire vehicles. EM shielding effectiveness is often an important consideration when specifying joint resistance, particularly when the joints are located over EM shielded electronic equipment bays.

Joint Breakdown Characteristics. The electrical breakdown properties of structural joining and fastening designs are important in determining the ability of the structure to carry lightning currents. Although it is relatively easy for a riveted aluminum structure to carry the full lightning current, it is much more difficult, if not impossible, to design an adhesively bonded aluminum or all-composite structure with this same current carrying ability. The joints and bonds between structural members in these vehicles

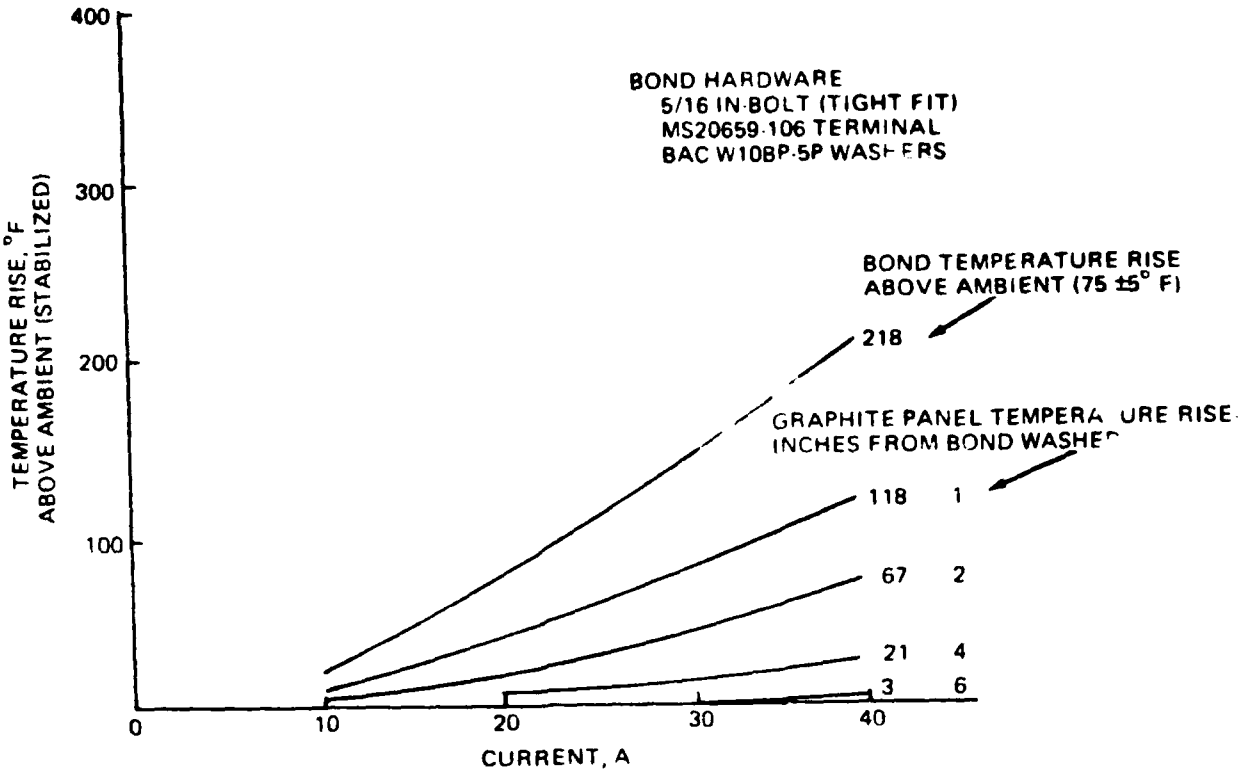

a. ELECTRICAL BOND GRAPHITE PANEL TEMPERATURE/CURRENT CURVES

Circuit breaker rating	Graphite panel plies	Bond configuration		Bolt torque in-lb	Bond temperature rise due to fault °F
		Bolt size	Washer size		
25	32	[a]3/16	Standard	20	20
25	32	[a]5/16	Standard	50	17
25	32	5/16	Standard	50	37
25	32	5/16	1.1 in^2	125	9

[a]Bolt thread into hole

b. BOND TEMPERATURE RISE DURING FAULT CLEARING

FIGURE 13. BONDING TEST RESULTS

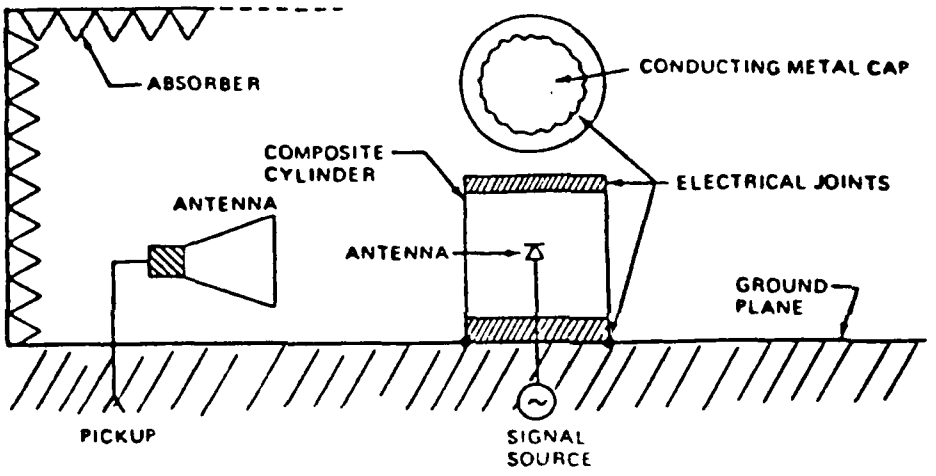

a. TEST SETUP

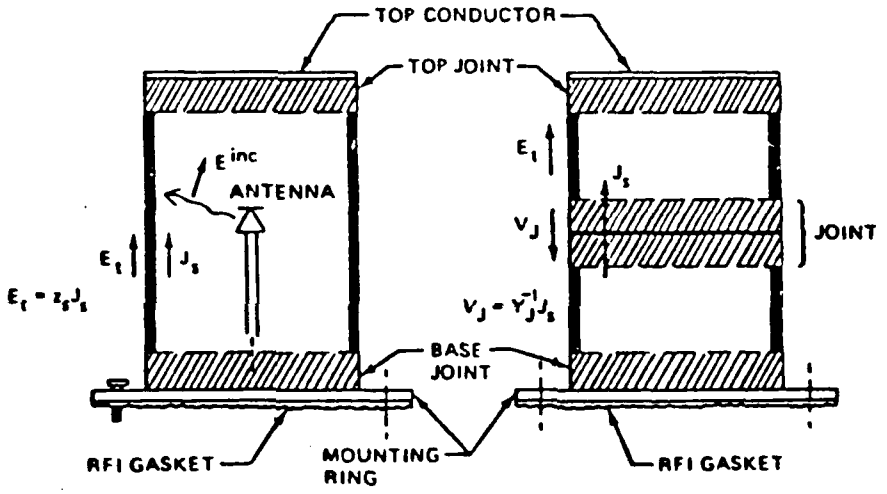

b. CYLINDRICAL SECTIONS

FIGURE 14. EXAMPLE OF SPECIAL SHAPES FOR JOINT CHARACTERIZATION

are essentially non-conducting material. Adhesively bonded structures typically use a non-conducting or poorly conducting epoxy material. Because of the high electrical stress during a lightning strike or electrical power system fault, arcs or sparks may develop in joints and bonds in composite material structures. In addition, composite material structures may be weakened from the heat generated where high current concentrations occur. Metallic fasteners, and metallic foil or screen materials must be installed in ways that make good electrical contact into the conducting portions of the basic structural materials. The main technical issue is designing the current path through the structure without adding excessive weight. Present design approaches utilize the features of lightning strike zones to minimize the extent of the structure where increased conduction is needed. Although the structural materials at the entry and exit points of lightning current must carry the full severe current levels, other portions of the structure need only carry a small fraction of the total lightning current. Tests are conducted to determine the allowable or breakdown levels of current or voltage that may be tolerated on the specific joints and fasteners used within an a vehicle structure.

Electrical current breakdown tests are conducted on specially fabricated specimens of the structure to determine the ability of the structure to carry current. This test method is used for assessing conductive joining and fastening methods. Lightning related currents are applied to the specimens and the maximum current handling capacity is determined, by stepwise increase of the applied current until failures are observed. Figure 15 (from Reference 19) illustrates a test setup for this method. The electrical properties of conducting joints depend upon current concentration, heat generation rates, thermal conductivity, and pressures that may build up in the joint. Results of these tests vary considerably among samples, depending upon the coatings and treatment of the joint to control heat and pressure. An example of such data is shown in Figure 16 taken from Reference 19.

Voltage breakdown tests are conducted on non-conducting or poorly conducting joints to determine the voltage levels where sparks could occur. A voltage ramp generator is applied to the specimen to determine the level where sparks occur in the joint. This limits the voltage that may be tolerated on the portions of structure where the particular joint sample is utilized. Figure 17 (from Reference 19) illustrates the test setup. A typical result of this test is shown in Figure 18 (from Reference 19). Results of these tests strongly depend upon the sharpness of the edges on the metal parts. This is because the breakdown voltage between two contacts having sharp points is lower than for rounded points. The actual voltage depends upon the separation of the metal contacts as discussed in the Select Screening Test Candidates section of this report.

Complete Vehicle Tests. Complete vehicle or subassembly tests can be used to determine the local lightning environment at portions of a vehicle relative to the external lightning arc environment. If the subelement tests show failures at current levels below the severe threat lightning values, then tests on a complete vehicle may be used to show that the local current environment is below the failure current level of individual subelements. Alternatively, a large subassembly of a vehicle, such as an engine nacelle, may be tested where the lightning current can be accurately established. Figure 6 illustrates how the subsections are selected and Figure 7 describes the two tests used (from Reference 19).

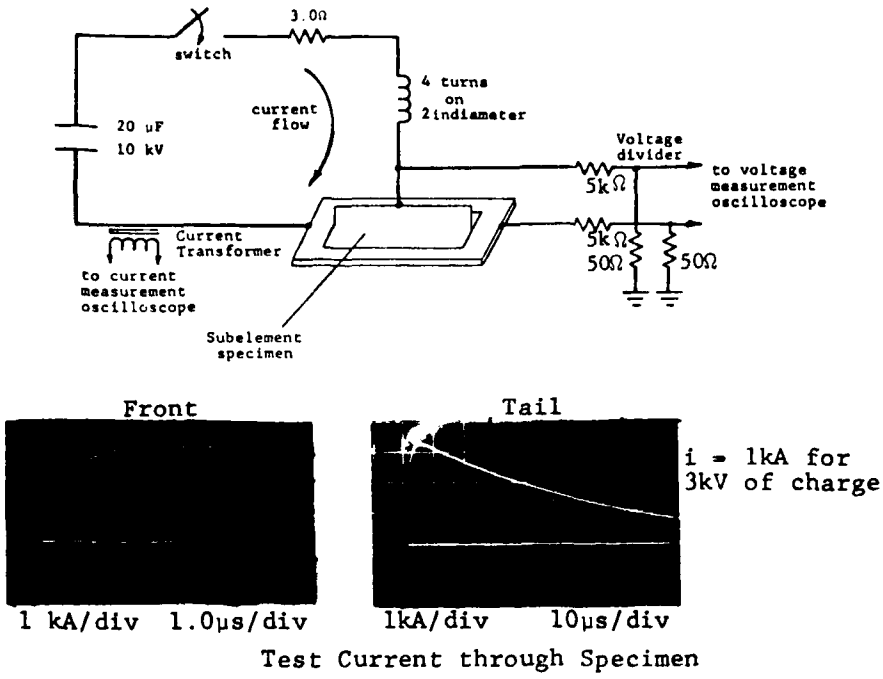

FIGURE 15. TEST CIRCUIT PARAMETERS FOR GENERATING THE 2 X 50 μs SIMULATED LIGHTNING CURRENT PULSE

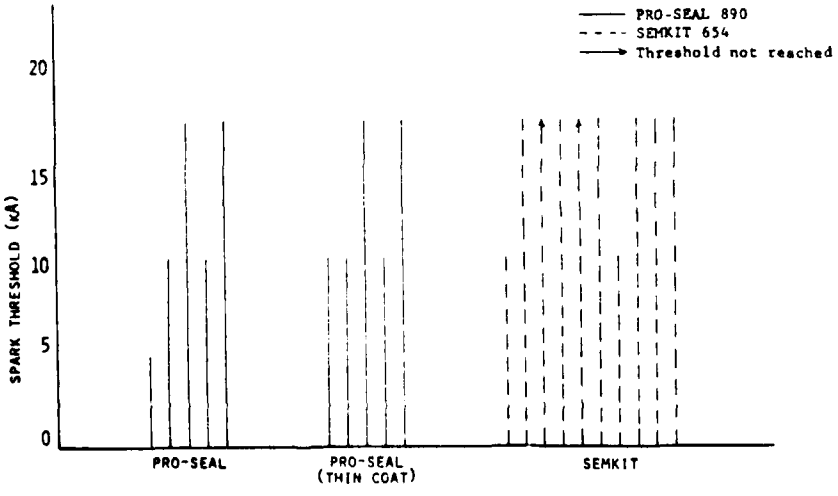

FIGURE 16. COMPARISON OF SPARK THRESHOLD LEVELS FOR VARIOUS SEALANTS APPLIED TO RIVET IN GR/EP LAMINATE SPECIMENS WITHOUT AN ADHESIVE CARRIER CLOTH.

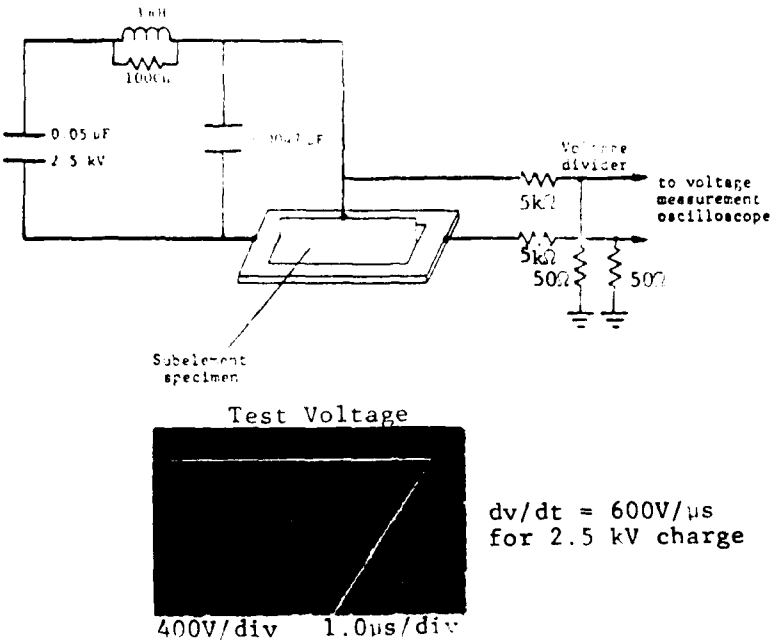

FIGURE 17. TEST CIRCUIT FOR APPLYING A CONTROLLED VOLTAGE RATE-OF-RISE TO SPECIMEN FOR DETERMINING ADHESIVE BREAKDOWN LEVELS

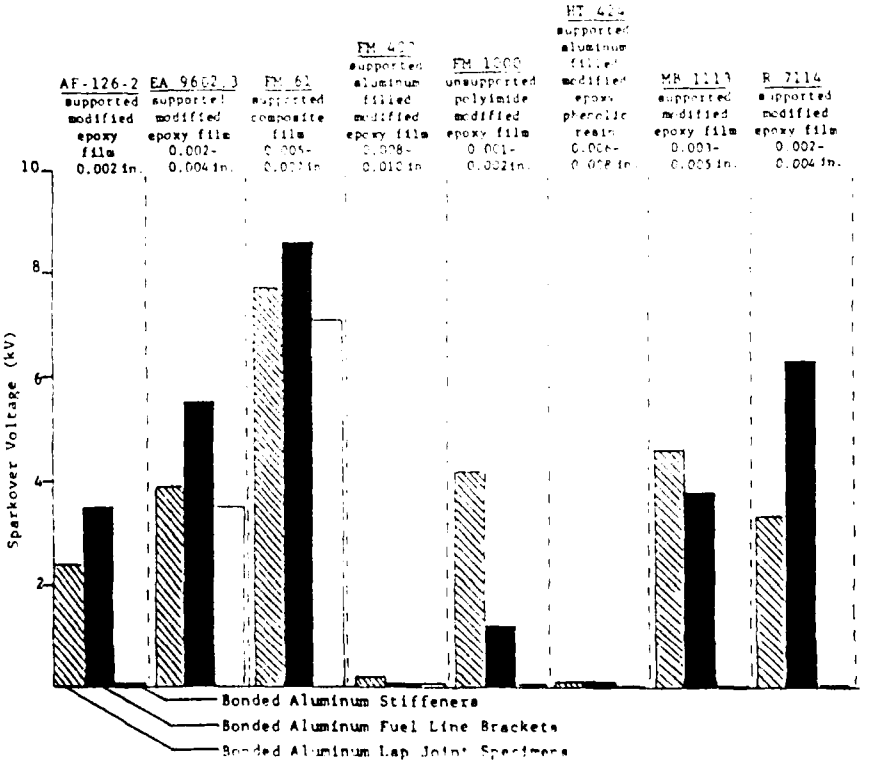

FIGURE 18. RANGES OF SPARKOVER VOLTAGES FOR BONDED ALUMINUM SPECIMENS

SELECT SCREENING TEST CANDIDATES.

This subsection discusses considerations used in selecting candidate bonding and grounding systems for the modeling, test, and evaluation described in the Analytical Models section of this report.

The candidate systems selected must fit into the emerging lightning protection design approach for advanced technology structures. Hence, the tests on the systems must provide direct measurement of electrical conditions at critical locations in the structure where sparking or severe electrical stresses exist on electronic components. As for example, where sparking on access doors or fuel gage electrical components could cause fuel ignition.

In most cases the lightning protection design for advanced aircraft structures is achieved by an iterative process, starting early in the design according to the following steps:

a. Determine the lightning strike zone(s) appropriate to the location of the structure.
b. Establish the local lightning threat environment for the structure.
c. Identify structural systems, subsystems, or components that may be susceptible to hazardous effects from lightning threat level currents or fields.
d. Establish the degree of protection required to reduce the local environment below the threshold of susceptibility.
e. Proceed with the protection design to achieve the needed margin of safety.
f. Verify the adequacy of the design by analysis and test.

The above design process requires many new considerations for advanced structural materials, because prior design experience from metal aircraft is not applicable for the new range of vehicle threat environments. For instance, where previous generation aircraft had a few volts and amps internally, the new structures can have a few hundred to a few thousand of volts and amps (Reference 19 & 27, for example). The process is further complicated by the interdisciplinary considerations required because lightning effects are both electrical and physical. Thus structural, electrical, power plant, and avionics technologies are all involved in the protection design steps.

Design and certification test specifications are needed for the above general reasons. They are also needed because critical structural subelements are difficult to identify without a screening test of several subelements. This difficulty is due to the complexity and size required in any electrical model that will represent the electrical properties of the entire structure.

SECTION III - ANALYTICAL MODELS

SELECTION OF GROUNDING AND BONDING METHODS FOR ANALYSIS.

Based on our investigations into test methods described in the Test Methods Evaluation section of this report, analyses were conducted to define models to predict results for the special test methods used for composites - reported in J.A. Plumer's 1984 NASA report (Reference 19) and R. Force et al 1977 NASC report (Reference 22). There is a large body of experimental data on electrical properties of composite materials and joints in these two sources. This published data was used in this section for determining the accuracy of the models for electrical properties of materials and complex joining and fastening methods. Plumer's work emphasized the lightning arc spark hazards of composites. Although extensive testing was completed, the test methods have not been supported by analysis. Consequently, we selected for analysis the following three test techniques from Plumer's NASA work:

1. Sparking Thresholds of Subelements
2. Breakdown Voltage of Subelements
3. End to End Resistance of Composite Wing

The first two analytical techniques are needed for the verification that fuel tanks are arc/spark free. Because of non-linearities, tests will always be required for spark free tank design and development data, and for verification. Our initial modeling efforts, reported herein, indicate that lower bounds on the spark threshold currents can be established before testing of fasteners in composites. This analysis would benefit design certification.

The third technique selected for analysis involves determination of current flow in the entire structure. A current flow analysis is needed to establish stress levels at joints between structural members. Present analytical methods are lacking because a complete vehicle (or a full-scale subelement) is needed to establish the stress at individual joints. The analytical capability to predict currents in a complete structure from design allowables on joint resistances would support design and design verification. The main benefit provided by mathematically modeling currents flowing in a composite structure is to provide design trade-offs before the structure is completed. A prediction capability will also reduce the amount of developmental testing needed. Analysis may also help reduce the risk that retrofit design would be needed if the design and certification were based only on tests using full-scale parts.

Modeling includes evaluation and application of proven computer modeling methods from EM theory to the solution of the new problems of determining current flow in composite structures. The main focus is on solving for currents and voltages in composite structures for determining grounding and bonding parameters. The first efforts concern details of structural fasteners in composites. Subsequent analysis determines the current distribution in complete composite wing structures.

RESISTANCE MODELS FOR COMPOSITE MATERIALS FASTENING.

This section describes the results of an investigation into analytical modeling to determine the resistance of metal fasteners in composite panels. Resistance parameters are needed to determine the current flow in composite

materials because the resistance of a line of fasteners in a joint can be as great as the resistance of a one meter section of skin. The investigation utilized the following five methods to compare the accuracy of each model used:

1. Resistance Sheet Analog Models.
2. Solution of Poisson's equation using Green's functions.
3. Numerical Relaxation solution of the two dimensional Laplace's equation.
4. Solution of Maxwell equations by the Method of Images in one dimension.
5. Solution of Maxwell equations by the Method of Images in two dimensions.

These five methods have been found useful for many other EM problems and are current technology. The application to gr/ep materials with metal fasteners has not been reported elsewhere in a consistent way useful to this program. The details of each analysis technique are given in more detail in Appendix B.

Results of this work have so far been very encouraging; a summary of the results is given in Table 9.

TABLE 9

SAMPLE RESISTANCE COMPARISON FOR DIFFERENT ANALYSIS METHODS

SAMPLE NO.*	RESISTANCE PAPER	GREEN'S FUNCTION	NUMERICAL RELAXATION	2-D IMAGES	1-D IMAGES
1	.0479	.0465	.0458	.0786	.0454
2	.0276	.0246	.0256	.0320	.0188
3	.0791	.0653	.0712	.1460	.0579
A	.0237	.0252	.0258	.0314	.0232
B	.0461	.0465	.0401	.0509	.0370
C	.0244	.0270	.0210	.0244	.0255
D	.0338	.0333	.0378	.0653	.0334
E	.0367	.0352	.0373	.0489	.0334

* DIMENSIONS GIVEN IN TABLE 10.

Each of the analytical methods listed above, and briefly described below, was tested on eight samples. The sample panel sizes were chosen in two ways. Samples 1-3 were chosen to agree with test panels measured by Plumer (1984). Samples A-E were chosen to test various fastener placements on the panel, and the shape of the panel.

Resistance Sheet Analog Method. This method used sheets of graphite paper cut to various rectangular dimensions shown in Figure 19 and Table 10. One edge was painted with a silver metal paint to establish an equipotential surface. This paint provides a resistance of 0.1 to 1 ohm per square for a typical brushed on thickness. The fastener was modeled as a circle of silver paint of various dimensions. An ohmeter was used to measure the resistance between the fastener and the edge of the sheet. Since the sheet is measured to be 2,000 ohms per square, the results were scaled to gr/ep with a conductivity of 28,000 and varying thicknesses (either four or seven ply). These values were chosen from Plumer's 1984 report containing various fastener tests. The limitations of this method are due to the anisotropy of the paper (1-2% according to Reference 35) and to the inability to paint accurate fastener sizes on the paper. However, these limitations should introduce errors of only a few percent.

Green's Function Solution. The solution of Poisson's equation with a charge located at the fastener center can be written using a Green's function technique. The boundary conditions on the sample are that the potential is zero on one edge (corresponding to the painted edge on the graphite paper), and that the tangent electric fields are zero on the other edges of the graphite paper. The solution can be written as an infinite sum of eigenfunctions normalized to a known potential at the fastener position. The resistance of the sample is found by integrating the electric field across the edge with zero potential. The current flowing across the edge is calculated using Ohm's law and the resistance found from the ratio of applied potential to current at the edge. Comparison between this method and the other techniques are shown in Table 9. The Green's function method shows excellent agreement with the resistance analog method. This method is easy to use and has a very fast numerical convergence. A possibly large source of error is due to the assumption that the fastener is modeled as a point source. If the fastener size becomes large compared to the panel size, then this error is quite large. However, for the cases considered, the fastener size limitation was not significant.

Numerical Relaxation. Solution of Poisson's equation using numerical relaxation techniques is a standard technique for solving many irregular geometrical problems that are not easily solved analytically. The technique used here is the Liebmann Iteration method (see Reference 35). Residuals to Laplace's equation are found at each grid point and potentials are readjusted to reduce the residuals. This is an overrelaxation method which convergences much faster than the ordinary relaxation methods. The limitations to this method are the quickness of the convergence which can be a problem for some geometries (fortunately not for the cases analyzed here), and the limitations due to grid size especially relative to the fastener size. We found that changing the grid size by a factor of two changed the calculated resistances by up to 10% for small fasteners, and by up to thirty percent for large fasteners. It is recommended that different grid sizes be used when applying this method to bound the error from an initially selected grid.

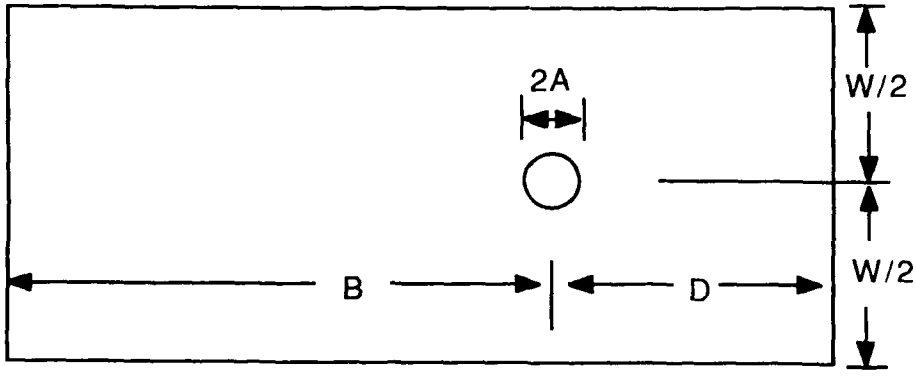

FIGURE 19. SAMPLE GEOMETRY WITH FASTENER

TABLE 10

SAMPLE DESCRIPTIONS DIMENSIONS (INCHES)

SAMPLE	D	B	W	A	t
1	1.10	5.0	3.0	0.06	0.056
2	0.75	5.0	3.0	0.20	0.100
3	9.00	9.0	3.0	0.25	0.056
A	2.00	1.9	3.0	0.05	0.056
B	0.05	3.9	3.0	0.05	0.056
C	0.50	3.4	6.0	0.05	0.056
D	4.70	3.4	3.0	0.05	0.056
E	0.50	3.4	3.0	0.05	0.056

NOTE: SAMPLES 1-3 are similar geometry to test fastener samples prepared and reported by Plumer (1984).

SAMPLES A-E were analyzed to test the various models as a function of sample geometry.

Variable dimensions are defined in Figure 19.

Method Of Images 2-D. The method of images is used in statics to solve boundary value problems only for simple geometries. For two or more parallel boundaries, an infinite number of images must be used to satisfy the boundary conditions. For the cases analyzed here using rectangular strips, an infinite number of images is needed in two dimensions. Convergence with this method is not reliable even for very large numbers of terms. The answers obtained from this method best agreed with the other techniques when only four images were used, one to satisfy each edge. If more than this were used, the answers were radically different from the other predictions due to convergence problems. Agreement with the previous techniques described is still spotty. Samples 2, A, B, C agree fairly well. Samples 1, 3, D, and E are up to a factor of two different. This technique was tried because it should handle the fastener size better than either the Green's function technique or numerical relaxation technique. This does not seem to be the case however, because of round-off errors from adding the large number of terms needed in the summation. This technique was the least reliable for calculating fastener resistance in a panel.

Method Of Images, 1-D. Due to the convergence problems of the 2-D method of images technique, one dimensional analysis was tried. In this case, convergence was fairly rapid. Agreement with the other techniques was found when the fastener size was small. When the fastener size was large compared to the panel, the agreement was not as good as, for example in Samples 2 and 3. This method should work well for panels shaped like Sample C (very wide) where the side boundaries should not affect the results.

Conclusions On Resistance Models. Five techniques were presented here for the analysis of metal fasteners in graphite epoxy panels. Four of the methods were shown to agree for most cases. Results from the fifth method (2-D method of images) showed poor agreement. The major limitation on all these techniques arises from the relative fastener diameter compared with the panel size. Testing of fasteners in panels is recommended to be done in panels much larger than the fastener diameter for ease in understanding and prediction of the results.

The most reliable techniques for obtaining fastener resistance in a graphite panel were found to be (1) the resistance sheet model, good independent of fastener or panel size, (2) the Green's function solution, good for small fasteners in large panels, and (3) the numerical relaxation technique, suited for larger fasteners in any size panel. The analytic techniques, Green's function and numerical relation methods, are more applicable to circular or rectangular panel shapes while the resistance sheet method can be used for any shape.

SPARKING THRESHOLD MODELS.

Samples Selected For Analysis. Three graphite epoxy fastening samples, from experimental work reported by Plumer (Reference 19), were selected for analysis. These samples are typical for a general aviation airplane design, cover a range of fastening techniques and have a range of sparking thresholds. The first sample panel, shown in Figure 20, is a riveted joint between aluminum and graphite epoxy (gr/ep) thin skin material. The second panel, shown in Figure 21, is an access door dome nut in gr/ep skin material. The third panel, shown in Figure 21, is a fuel line feed-through in a gr/ep thin skin material to be used between wet and dry sides of a fuel tank.

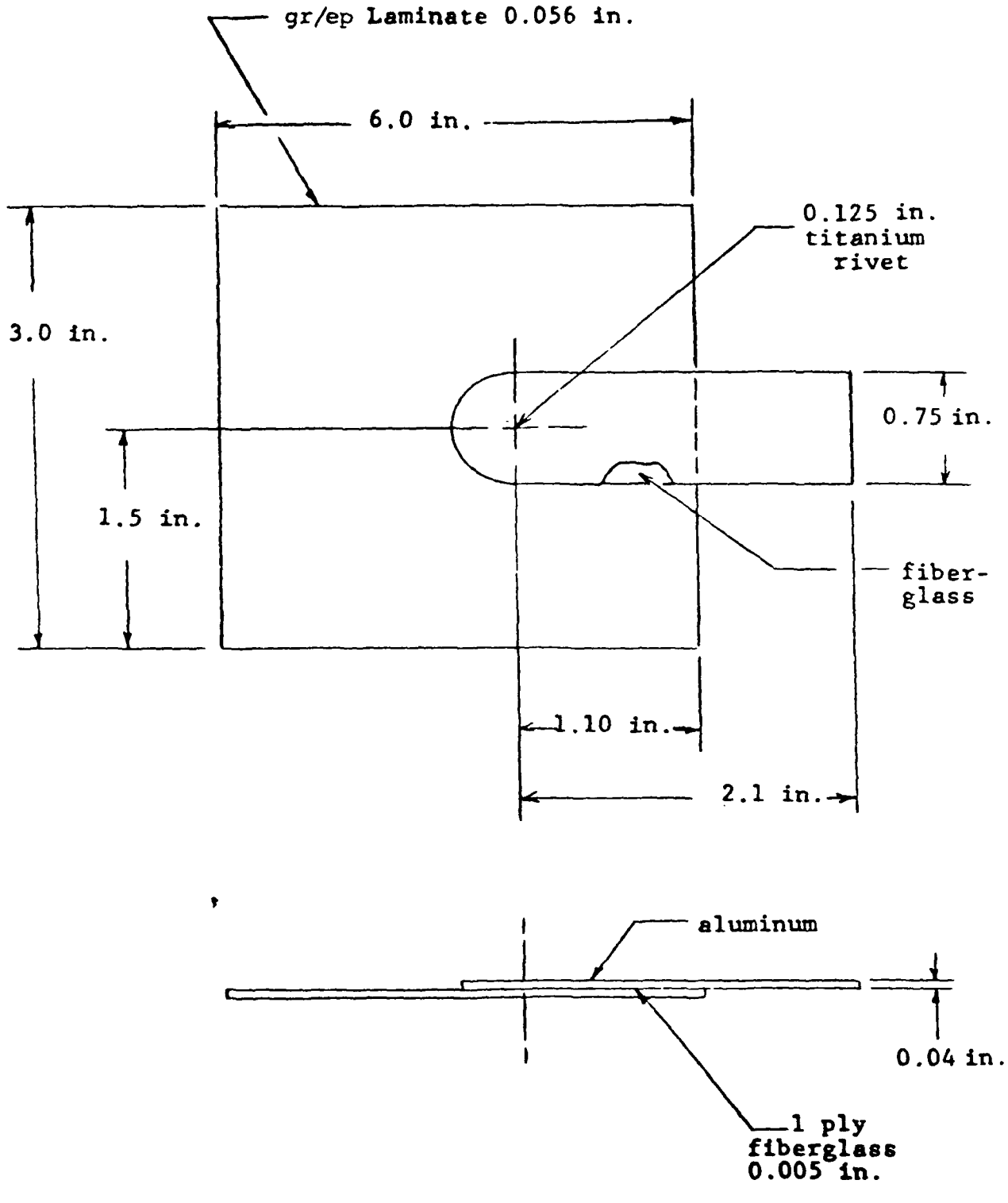

FIGURE 20. RIVET IN GR/EP LAMINATE TEST SPECIMEN

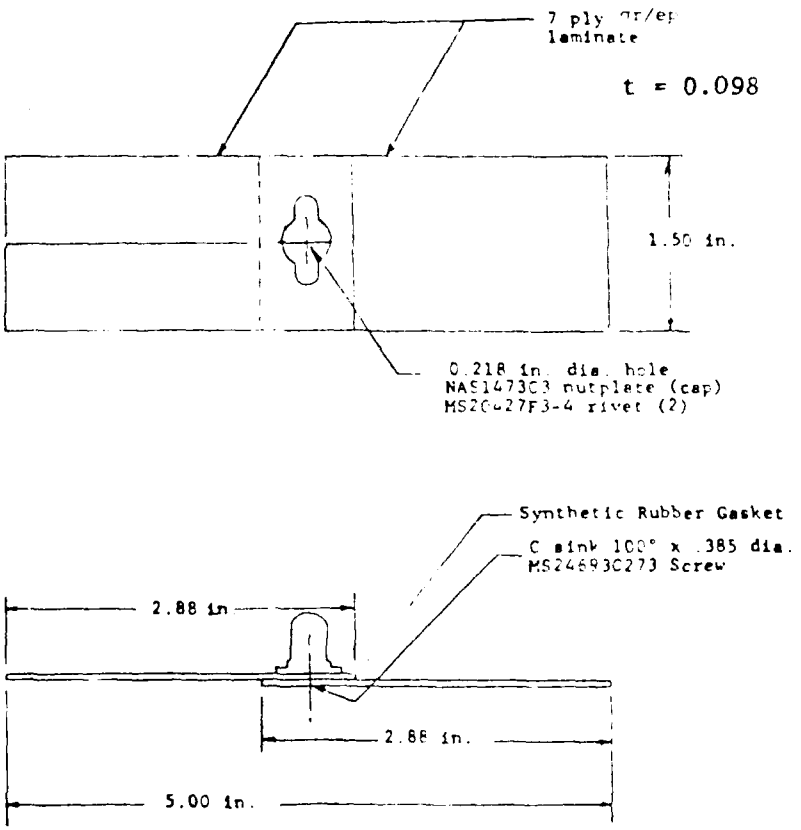

FIGURE 21. ACCESS DOOR DOME NUT IN GR EP LAMINATE

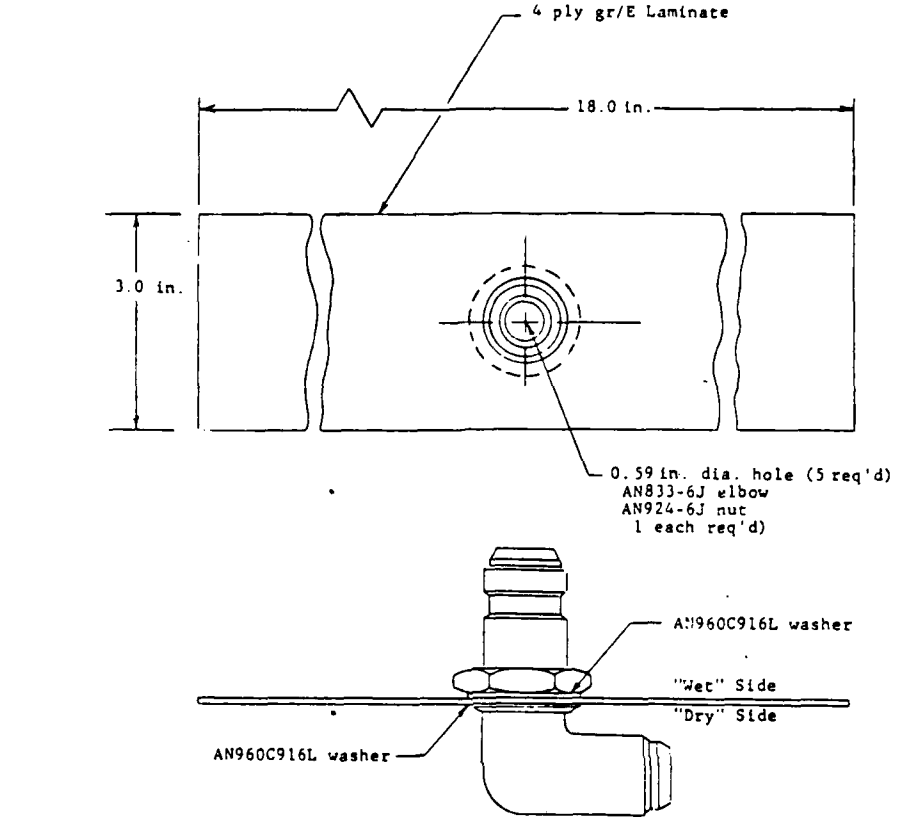

FIGURE 22. WET SIDE VIEW OF FUEL LINE FEED-THROUGH ELBÓW IN GR/EP LAMINATE

The electrical sparking parameters and comparison with the predicted thresholds for the three selected panels are shown in Table 11. When lightning currents are applied above the current threshold of the fastener samples, sparks will appear at the interface between the metal fasteners and the underlying gr/ep material. The current level for spark initiation depends upon the geometry of the fasteners, skin thickness and treatments applied to hold down the pressure build-up at the joint. The range of currents for sparks to initiate is from 2.5kA to 20kA depending upon which sample is tested. Figure 23 illustrates the sparks on sample number three at current just above the spark threshold level.

TABLE 11

DAMAGE MODEL COMPARISON

SAMPLE	MEASURED SPARK CURRENT THRESHOLD (k Amp)	PREDICTED FROM MEASURED CURRENT			PREDICTED MAX ACTION INTEGRAL (Amp^2 -sec)
		VOLTAGE DROP (Volts)	CURRENT DENSITY (Cirmil/Amp)	ACTION INTEGRAL (Amp^2 -sec)	
1	2.5-5	120-240	6-12	250-1000	390
2	5-10	140-280	8.5-17	1000-4000	3800
3	10-20	800-1600	6.6-13	3600-5800	8600

FIGURE 23. SPARK AT WASHER TO GR/EP INTERFACE RESULTING FROM A 15 kA CURRENT STRIKE TO THE FUEL FEED-THROUGH ELBOW. WET SIDE VIEW SHOWN.

Composite Material Damage Models. A damage model is needed to explain and understand the limitations on current flow at gr/ep joints. Several of the possible models are discussed in this section. One model that seems appropriate is to correlate the radius of physical damage on gr/ep test panels from lightning strikes to the size of the fastener. Estimates of physical damage to composite panels have been published to characterize the damage area from lightning strikes. Figure 24 shows the data from Fisher and Plumer (Reference 4). A second damage model that seems appropriate is to correlate the action integral of the current through the fastener with the surface area between the fastener and gr/ep material. The voltage drop on the fastener is also a possible limiting factor; this drop was calculated for the three samples using the resistances determined in the Resistance Modeling section. Finally, a simple model is formulated to correlate the peak current density at the fastener with the onset of sparks. Comparison of current thresholds based on these damage models with the experimental results indicate that both the simple model based upon current density at the fastener and the damage radius model are the best. These models will be discussed in the following sections.

Physical Damage Radius Model. A model for the physical damage caused by lightning currents in gr/ep materials was developed through extensive testing by the USAF, NADC, NASA and commercial companies. The body of knowledge on the tolerance of flat panels of gr/ep materials is well understood. The data shown in Figure 24, from Reference 4, describes the threshold for physical damage in terms of allowable action integral as a function of the number of plies of material. Three damage conditions are considered:

1. Superficial damage to outer plies only,
2. Deep penetration and damage within 10 cm of the arc,
3. Puncture and widespread damage.

The data in Figure 23 shows a correlation, as discussed below, between the composite material cross-sectional area and the action integral (integral of the square of the applied current over time). The relation is given by:

$$\text{Area}^2 = k \int I(t)^2 \, dt$$

where k is a proportionality constant obtained from Figure 24 by comparing the maximum action integral for non-degraded graphite with the area in square centimeters. Thus, for graphite

$$k = (.025 \text{ in})^2 / 2.E3 \text{ Amp}^2 - \text{sec} = 3.1 \text{ E-7 in}^2 - \text{Amp}^{-2} - \text{sec}^{-1}$$

Figure 24 shows that increasing the area by 10 times increases maximum action integral which the fastener can withstand by a factor of 100.

Calculation of the allowable action integral depends upon the area of material where current may flow; this requires consideration of the flow path. Current flow in a composite skin is confined to the general direction of current flow in the airplane structure; Figure 25 illustrates this concept. Thus the area for current flow is

$$\text{Area} = \pi rt$$

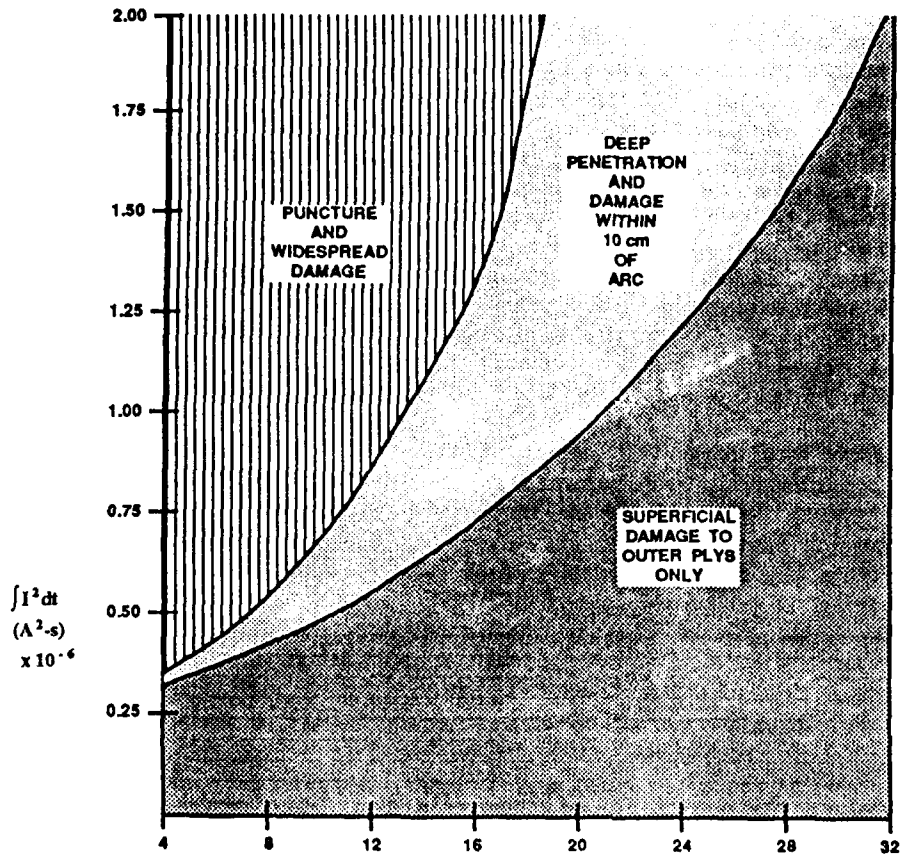

Estimated visible damage to unprotected graphite composites.
- For graphite composites, the damage extends only throughout the visibly damaged region.

COMPOSITE $\int I^2dt$ CONDUCTION CAPABILITY

Composite Cross-Sectional Area		$\int I^2 dt$ (A^2-s)			
		Boron		Graphite	
cm^2	in^2	Non-degraded	Degraded	Non-degraded	Degraded
0.016	(0.0025)	1	10		
0.161	(0.025)	10^2	10^3	2×10^3	2×10^4
1.610	(1.25)	10^4	10^5	2×10^5	2×10^6
16.100	(2.50)	10^6	10^7	2×10^7	2×10^8

FIGURE 24. COMPOSITE ACTION INTEGRAL CONDUCTION CAPABILITY

where r is the radius of the fastener and t is the thickness of the graphite or the depth of the fastener in the graphite panel, whichever is less.

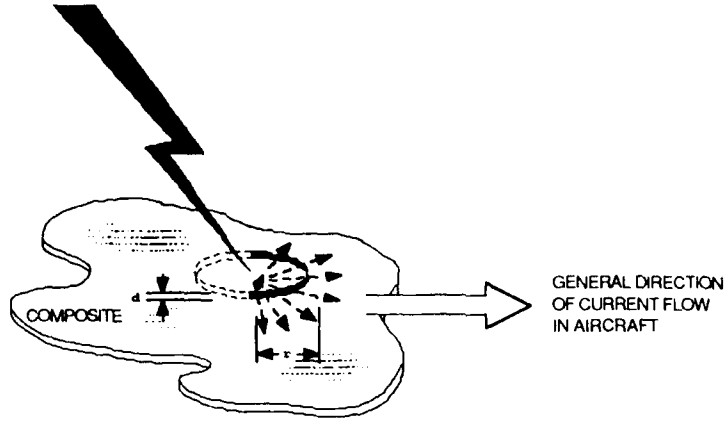

FIGURE 25. COMPOSITE THICKNESS VS. AREA OF DAMAGE FROM CONDUCTED CURRENT

The damage model assumes that the damage radius, for superficial damage, is equal to the fastener radius. Thus according to this model the maximum action integral for a fastener is

$$\text{Maximum Action Integral} = \text{Area}^2 / k$$

$$= (\pi r t)^2 \times 3.2 \text{ E+6 Amps}^2 - \text{sec}$$

where r and t are in inches. The predicted maximum action integral values for the three fastener samples under analysis are shown in the last column of Table 11. The predicted values are within the range of the measured action integrals as presented in column 5 of Table 11 for Samples #1 and #2 and slightly larger than the measured action integral for Sample #3.

Voltage Drop Model. One theory of sparking in composite material joints predicts that a spark will occur if the voltage has built up enough to burn a filament of graphite. To test this theory, the sample voltage drop may be predicted using the calculated resistance of the joints (from previous sections) and the measured values of sparking current threshold. The calculations presented in Table 11 were based upon the resistances determined by the resistance sheet analog method. If this theory was accurate, the predicted voltages for each fastener sample should be identical, instead there is over an order of magnitude variation in predicted voltages.

Current Density Model. A theory for the maximum current handling capacity of electrical equipment is based upon maximum current density. This theory assumes that hot spots build up at locations of maximum current density, and ultimately limit the maximum current handling capacity. This has been useful in the design of transformers and motor and generator power equipment; a rule of thumb is that 600 circular mils per ampere is a maximum for enclosed equipment. A guideline for lightning current diverters is that 0.05 circular mils per ampere is required for thin metal diverter strips. The current

density model calculations used the number of circular mils in the fastener and the measured sparking current thresholds; these numbers appear as circular mils per ampere in the model and experimental data tabulation in Table 11. The results show only a factor of two to three variation between the values predicted using this model for the three fastener samples. This model should predict a constant value useable for all fasteners.

Damage Model Conclusions. The predicted current density data indicates a strong correlation between the sparking current threshold and the maximum current density in the fasteners. Designs having at least 20 circular mils per ampere should pass spark free. These results are very preliminary, being based on so few samples, but it appears that a test program or additional analysis of experimental data would be warranted. Should so simple a guideline prove to be generally applicable, it would have a great effect on the design and certification process. A possible rationale for the success of this model is because there is a fundamental limit on current handling capability of gr/ep resulting from the phenomenon of sequential burnout starting with the individual graphite fibers. Since each of the graphite fibers carries a small portion of the total current, when some reach their current burnout limit, then the others will increase their share of the total current leading to an avalanche failure of the remaining fibers. The number of fibers available depends upon the area of the fastener junction to the base material. Hence the sparking threshold current limitation is based upon current density at the fastener interface to the gr/ep panel.

There is also good correlation between the predicted maximum action integral and the action integral calculated from measured sparking currents and lightning waveforms. For the range of parameters in Table 11, the maximum action integral model agrees well with the measured value. This model overestimates the ability of the larger fastener, Sample #3, to withstand sparking. Better measurement of the empirical relation between action integral and fastener contact area with gr/ep panels is necessary.

The correlation between sparking thresholds and calculated voltages on the joints is not good. The largest voltages were on the largest sample where the main portion of the voltage was from the bulk material and not from the joint between the fastener and skin material. The data indicates that a voltage drop of 50-100 volts should be tolerable in conducting electrical bonds between portions of graphite composite structure.

It should be noted that the samples selected for analysis were not treated to increase the tolerance to pressure build-ups at the fastener/composite joints. Proper joint treatments can increase the sparking thresholds by an order of magnitude. These treatments include epoxy adhesives, precast solid plastic caps, and sealants. The art of designing these treatments is evolving with aircraft applications of composite materials. Because the weight savings from using composites may be negated by the added materials for lightning protection, research should continue into special light weight joint treatments. The certification data for these should always include test results. The analysis models discussed previously should be useful for eliminating joint test candidates where the current levels are well below sparking thresholds. Using these models may reduce the amount of testing required. Analysis is not a suitable replacement for tests on lightning critical items, however.

BREAKDOWN VOLTAGE OF SUBELEMENTS.

Samples Selected For Analysis. Data in Reference 19 describes samples of adhesively bonded aluminum joints that were tested to determine the break down voltages. The samples were simple lap joints bonded over a 1 inch square area at one edge. A number of different adhesive bonding materials were used to join the samples. A series of tests was run on samples of one adhesive and specimens with carefully prepared edges to remove burrs. The need to remove burrs was prompted by earlier testing where several conducting joints were found, although the adhesive was non-conducting. The breakdown voltage versus bondline thickness, shown in Table 12, shows a wide variation. For thin bonds the breakdown voltage is about 400 volts per mil (0.001 in.) thickness. For thicker bonds the voltage required to cause sparkover reduces to about 200 volts per mil. All the breakdowns occurred at the edges of the samples, indicating that the adhesive dielectric withstand voltage is greater than that of air.

Table 12

Breakdown Voltage vs. Bondline Thickness
(AF-126-2 Adhesive Only from Ref. 19)

BOND LINE THICKNESS (Inches)	BREAKDOWN VOLTAGE (Volts)	(Volts/Mil)
0.0035	1200-2400	340-380
0.0070	2400-2800	340-400
0.0100	3600-4700	360-470
0.0150	4000-4800	270-320
0.0200	4000-4800	200-240

Table 13

Breakdown Voltage Of Fuel Line Bracket Specimens

ADHESIVE DESCRIPTION			RANGE OF BREAKDOWN VOLTAGES (KV)
DESIGNATION	TYPE	CONDUCTIVITY	
AF-126-2	SUP.	NONE	1.8-3.5
EA 9602.3	SUP.	NONE	<0.1-5.5
FM 61	SUP.	NONE	1.0
FM 400	SUP.	PARTIAL	0.5-10.0
FM 1000	UNSUP.	NONE	0.2-10.0
HT 424	SUP.	PARTIAL	0.1-10.0
MB 1113	SUP.	NONE	0.2-5.0
R 7114	SUP.	NONE	0.5-2.0

A second series of tests was done on the breakdown voltage of aluminum fuel line brackets bonded to an aluminum plate using a series of different adhesives; the data (from Reference 19) is shown in Table 13. The bondline thickness of these samples was not carefully measured but was estimated to be from 0.005 to 0.020 inches. All the brackets had been carefully deburred and later checked to see that the joint was non-conducting (or at least poorly conducting for the joints with conductive adhesive). The range of breakdown voltages for these brackets, shown in Table 13, varies so much that distinctions among the adhesives are not apparent.

Voltage Breakdown Model. The model of voltage breakdown is an old one that is well proven for spark-gaps. A reference to the model is made in several places, for instance Reference Data For Radio Engineers, Sams Publishers sixth edition p. 48-2: "An approximate rule for uniform fields at frequencies up to at least 300 MHz is that the breakdown gradient of air is 30 peak kilovolts per centimeter or 75-peak kilovolts/inch at sea level and normal pressure. The breakdown voltage is approximately proportional to pressure and inversely proportional to temperature." Figure 26 illustrates the above variation with temperature and pressure as well as the variations between sharp points and spheres. This model indicates that the breakdown voltage should be between 25 and 75 volts per mil of bond line. This is not inconsistent with the observed minimum voltage breakdown levels with the fasteners and brackets. The adhesive layer may increase the breakdown voltage because of increased dielectric strength for some of the adhesive materials. This should be used with caution however, because the voltage breakdown decreases with altitude; at 20,000 feet the breakdown voltage is approximately 1/2 that at sea level.

Voltage Breakdown Model Conclusions. The results of the breakdown model investigation indicate that at least some of the breakdown during test was because of air breakdown for the short gaps. Although some of the samples tested had higher levels of breakdown threshold, the treatment of the edges with adhesive was not well enough controlled to provide the same level of protection for all samples. The use of dielectric layers to increase the breakdown levels for bonded structures is an important area where further research may improve the manufacturing methods.

STRUCTURE RESISTANCE MODEL.

Current Modeling Capability for Composite Structures. The electromagnetic coupling modeling for lightning protection design must account for the composite materials and the fastening & joining techniques for advanced technology aircraft. A considerable base of analysis is available from prior research and development to apply for this effort. These techniques are summarized in the AEHP program documentation, earlier work of the Naval Air System Command, and of the Air Force Flight Dynamics Laboratory. References to these documents are included in Appendix A.

The present modeling techniques for metal aircraft need to be modified in several ways for application to the test bed analysis. The principal elements of the modeling and analysis, shown in Figure 27, follow the flow of energy from external environments to the internal equipment. Many of the present models are directly useful, such as the environment, external response, cable and wiring and, internal equipment. The penetration-to-interior models require changes for particular aircraft and wiring configurations.

Sparkgap breakdown voltages

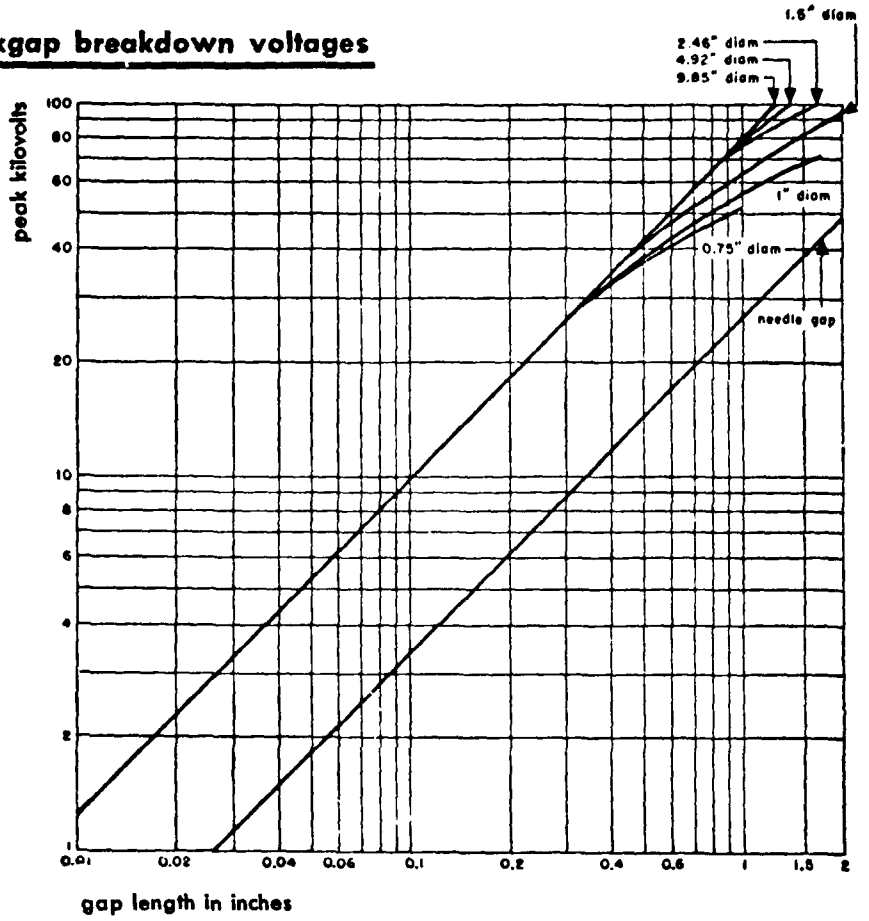

Table of multiplying factors.

pressure		temperature in degrees centigrade					
In Hg	mm Hg	−40	−20	0	20	40	60
5	127	0.26	0.24	0.23	0.21	0.20	0.19
10	254	0.47	0.44	0.42	0.39	0.37	0.34
15	381	0.68	0.64	0.60	0.56	0.53	0.50
20	508	0.87	0.82	0.77	0.72	0.68	0.64
25	635	1.07	0.99	0.93	0.87	0.82	0.77
30	762	1.25	1.17	1.10	1.03	0.97	0.91
35	889	1.43	1.34	1.26	1.19	1.12	1.05
40	1016	1.61	1.51	1.42	1.33	1.25	1.17
45	1143	1.79	1.68	1.58	1.49	1.40	1.31
50	1270	1.96	1.84	1.73	1.63	1.53	1.44
55	1397	2.13	2.01	1.89	1.78	1.67	1.57
60	1524	2.30	2.17	2.04	1.92	1.80	1.69

FIGURE 26. SPARKGAP BREAKDOWN VOLTAGES

Protection Analysis Elements For Air Vehicles

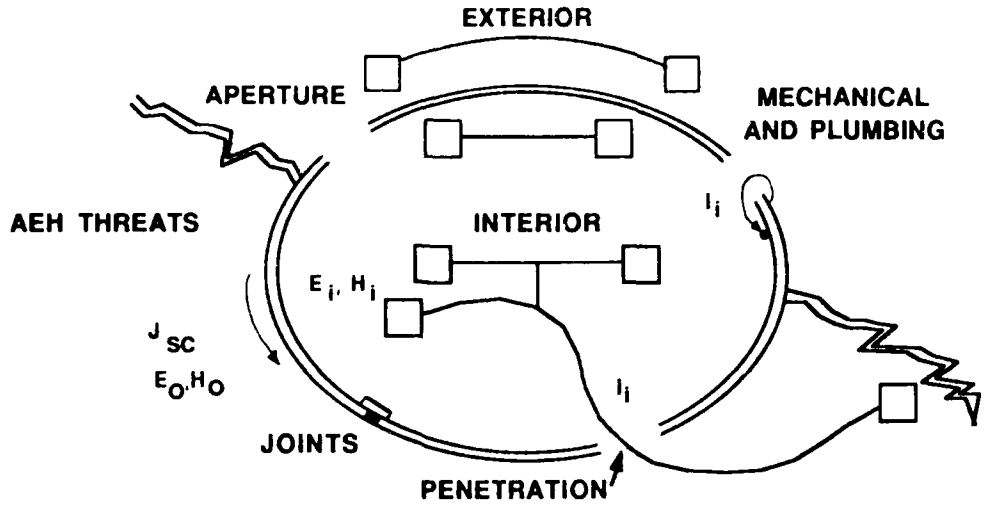

EM ANALYSIS	RESPONSE VARIABLES	PREDICTION TOOLS COMPUTER	HAND CALCULATIONS
THREAT MODEL	$I, i Z_C$	X	X
STRUCTURAL INTERACTION	J_{SC}, E_O, H_O	X	X
SHIELDING	Z_S, E_i, H_i	X	X
PENETRATIONS	V_{oc}, Z_C, E, H	X	X
FIELDS TO WIRE	V_{oc}, I_{SC}	X	X
WIRE TO WIRE	V_{oc}, I_{SC}, Z_m	X	X
WIRE TO BOX	V_L, I_L, Z_{BOX}	X	X

FIGURE 27. PROTECTION ANALYSIS ELEMENTS FOR AIR VEHICLES

The modeling of energy penetration from the exterior to the interior has several common elements particularly in the apertures and exterior wiring and cables. The principal difference between metal and composite aircraft lies in the increased contribution of the resistive voltage drop (IR) in the fuselage and wing skins, and in the increased current flow paths in the structure. This is because the gr/ep structure has typically 1000-3000 times higher resistance than the similar aluminum structure. For frequencies above a few megahertz, or early time (i.e. for a few microseconds), there is no difference in lightning response between aluminum and graphite structures. This is because at high frequencies, electromagnetic "skin-effect" forces the currents to the outside of the materials, to the outside surfaces, and to sharp radius of curvature portions of the structure. Protection against the early pulse is essentially the same for both structural materials: keep wiring near metal or structure to reduce the magnetic field B-dot coupling factors.

The main difference in energy penetration between graphite and aluminum structures is in the frequencies below the megahertz range, or late time (i.e. for a few tens of microseconds). For this range of frequencies (or late time in to a lightning pulse) and as a result of the range of thicknesses and materials used in aircraft structure, considerable current flows into the interior. Since the current flow is resistive for graphite epoxy materials, the protection measure of keeping the wiring close to structure will not have any protective effect. Furthermore, the IR voltage drop will be much larger for gr/ep than for aluminum.

Composite Wing Model. A dc resistance model of the wing composite used in the NASA tests was constructed to determine the amount of current flowing through various sections of the wing. The results of this modeling study will predict energy flows into various structural members and fasteners. A dc model is appropriate for lightning studies since structural and fastener damage occurs from the high energy levels which are mainly from large low frequency components of the lightning pulse.

An estimate of the dimensions and properties of the composite wing are listed in Table 14. The spars were considered "I" beam sections 1/4" thick with the remaining values given in the Table 14. The skin was taken as a product of average dimensions obtained from Plumer's NASA report (Reference 19). Both sides of the wing skin were considered in the total area. The braid running in the leading wing edge was assumed to be 1/2" braid which was taken to have 3 milliohm/meter resistance, as measured in previous studies. Fasteners were assumed to have a resistance of 10 milliohms per fastener. These resistances are similar to other predictions we have done for determination of various fastener resistances.

This simple resistance model predicts current level as percentages of total current in Table 14. These are compared to Plumer's measured values for late time (80 microseconds) into the pulse. The agreement is good considering that dimensions, conductivities, number of fasteners, and fastener resistances are not accurately known.

Bellanca Test Bed Model. The Bellanca test bed has been designed with consideration for protection of the internal equipment against internal currents and fields. First, the entire structure has been provided with a current path for the low frequency, late time lightning currents. This current path has gr/ep structure augmented with aluminum foil and screen.

TABLE 14

COMPOSITE WING RESISTANCE MODEL RESULTS VS. MEASUREMENT

ITEM	WIDTH (IN)	HEIGHT (IN)	AREA (IN^2)	CONDUCTIVITY (MHO/M)	STRUCTURE RESISTANCE (OHM)	TOTAL FASTENER RESISTANCE	STRUCTURE RESISTANCE W/FASTENERS	ITEM CURRENT (% OF TOTAL)	MEASURED CURRENT (6) (% OF TOTAL)
FRONT SPAR	1.00	2.00	0.88	28000	0.363	0.005 (1)	0.368	3.4	2% TO 5%
CENTER SPAR	2.50	5.00	2.38	28000	0.134	0.005 (2)	0.139	9.0	2% TO 5%
REAR SPAR	1.50	3.00	1.38	28000	0.231	0.005 (3)	0.236	5.3	2% TO 5%
SKIN	77.00	0.0875	6.74	28000	0.047	0.001 (4)	0.048	25.8	29%
BRAID	-				0.017	0.005 (5)	0.022	56.6	71%

FOOTNOTES:

(1) 2 FASTENERS ASSUMED
(2) 2 FASTENERS ASSUMED
(3) 2 FASTENERS ASSUMED
(4) 10 FASTENERS ASSUMED
(5) 2 FASTENERS ASSUMED
(6) MEASURED DATA FROM PLUMER (1984)

TOTAL RESISTANCE
OF STRUCTURE = 0.012 OHM

FASTENER RESISTANCE
ASSUMED = 0.01 OHM

This design is intended also to improve the grounding and bonding of the electronic equipment and wiring.

A resistor network model is used to determine the end-to-end connectivity of the test bed structure. This model may also be used to determine the late time currents (greater than 10 microsecond for lightning) that may be potentially damaging to the structure.

The test bed current paths, shown in Figure 28a, are modeled by the resistor network shown in Figure 28b. The values for these resistors determine the current flow. In a design project, developmental tests would be carried out to determine these parameters before implementing the design. For the test bed, the design and implementation has been combined somewhat. This is partly to reduce costs and partly due to the one of a kind nature of the test bed. The Bellanca aircraft that the test bed is modeled after has not been protected against lightning yet, so that the developmental testing data is not available. The fastener resistance values allow for a number of fasteners in parallel.

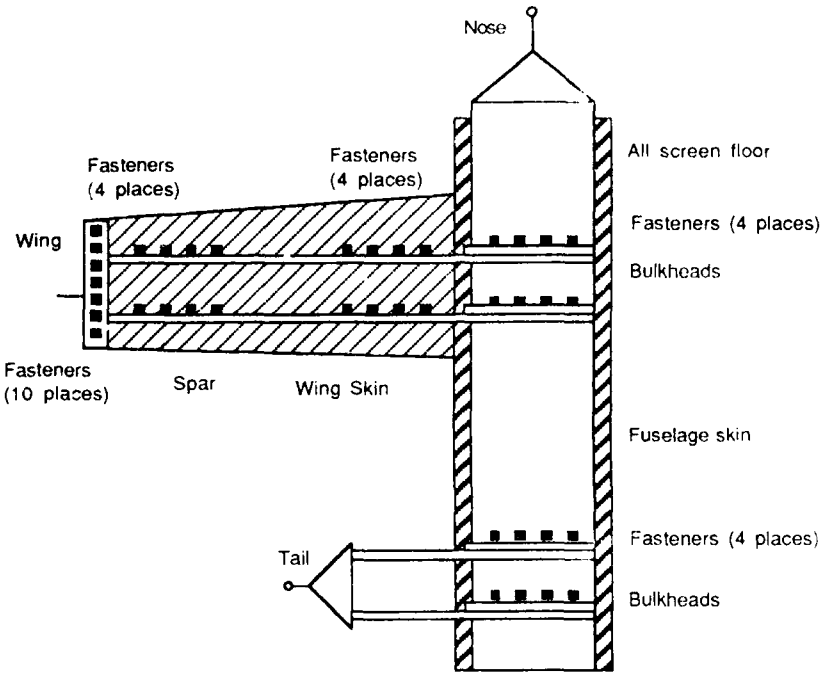

a. SCHEMATIC LAYOUT OF TEST BED

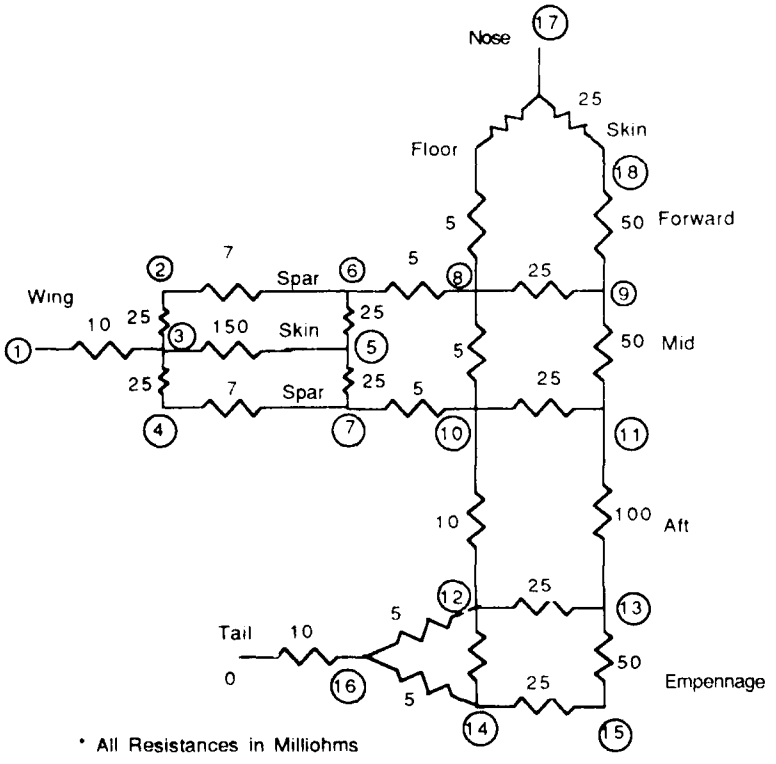

b. RESISTOR MODEL

FIGURE 28. TEST BED CONFIGURATION AND RESISTOR MODEL

APPENDIX A

REFERENCES

A.1 General

1. "International Aerospace and Ground Conference on Lightning and Static Electricity" (8); Fort Worth, Texas; AD-A135 100; June 21-23, 1983.

2. IEEE Electromagnetic Compatibility Society; Special Issue on Lightning and Its Interaction With Aircraft; "IEEE Transactions on EMC"; Volume 24, No. 2; May 1982.

3. Plumer, J.A. and Robb, J.D.; "The Direct Effects of Lightning on Aircraft"; IEEE Transaction on EMC, Vol. 24, No. 2; May 1982.

4. Fisher, F.A. and Plumer, J.A.; "Lightning Protection of Aircraft"; NASA RP-1008, 1977.

5. Blake, L. and Corbin, Jr., C.; "Electrical/Electromagnetic Concerns Associated with Advanced Composite Materials in Aerospace Systems"; AGARD Paper No. 283; 1979.

6. Military Standard MIL-STD-1757; "Lightning Qualification Test Techniques for Aerospace Vehicles and Hardware"; June 17, 1980.

7. Military Specification MIL-B-5087B(ASG); "Bonding, Electrical, and Lightning Protection, for Aerospace Systems"; Amendment 2; August 31, 1970.

8. Federal Aviation Administration - Florida Institute of Technology; "Workshop on Grounding and Lightning Technology; March 1979.

9. Federal Aviation Administration - Georgia Institute of Technology; "Workshop on Grounding and Lightning Protection"; FAA-RD-78-83; May 1978.

10. Radgowski, E. and Albrecht, R.;"Investigation of Electrostatic Discharge in Aircraft Fuel Tanks During Refueling"; Paper 78-1501 at the AIAA Aircraft Systems and Technology Conference, Los Angeles, California, August 21-23, 1978.

A.2 Advanced Aircraft & Lightning Protection

11. Heiderscheidt, G.A.; "Protecting the World's Largest Commercial Helicopter from Atmospheric Hazards"; 'International Aerospace and Ground Conference on Lightning and Static Electricity (8th)'; 1983.

12. Doggett, P.A.; "Lightning Protection Design and Lightning Threat Flight Clearance of a Fly-by-Wire Flight Control System for an Unstable Aircraft"; 'International Aerospace and Ground Conference on Lightning and Static Electricity (8th)'; 1983.

13. Evans, R.H. and Bishop J.; "Induced Transients in a Simulated Lightning Test of the Fly-by-Wire Jaguar Aircraft"; 'International Aerospace and Ground Conference on Lightning and Static Electricity (8th)'; 1983.

A.3 Advanced Structures Protection

14. National Technical Information Service; "Adhesive Bonding of Composite Materials"; 1966-January, 1984 (Citations from the Metals Abstracts Data Base) NTIS PB84-858133; January 1984.

15. National Technical Information Service; "Adhesive Bonding of Aluminum and Aluminum Alloys"; 1970-1983 (Citations From the Engineering Index Data Base); NTIS PB84-856426; December 1983.

16. National Technical Information Service; "Adhesive Bonding of Composite Materials"; 1970-1983 (Citations for the Engineering Index Data Base); NTIS PB 83-859660 December 1983.

17. Amason, M.P. and Hofmeister, M.C.; "Lightning Spark Barrier"; 'International Aerospace and Ground Conference on Lightning and Static Electricity' (8); 1983.

18. Roberts, R.H.; "Advanced Development of Conceptual Hardware for the Lightweight Fighter"; Technical Report AFFDL-TR-77-67; October 1977.

A.4 Test Methods/Test Data

19. Pryzby, J.E. and Plumer, J.A.; "Lightning Protection Guidelines and Test Data for Adhesively Bonded Aircraft Structures"; NASA Contractor Report 3762, January 1984.

20. East, D.A. and Geren, W.P.; "Application of the Swept CW Measurement Method to the Prediction of Transients Induced in Aircraft Wiring by Lightning"; IEEE International Symposium on Electromagnetic Compatibility; 1981.

21. Olson, G.O. and Schneider, S.D.; "Graphite/Epoxy Wing Box Fuel Ignition Investigation" Final Technical Report; NASC contract N00019-80-C-0597; January 1984.

22. Force, R., Geren, P., Strawe, D., Schmidt, A.; "Investigation of Effects of Electromagnetic Energy on Advanced Composite Aircraft Structures and Their Associated Avionic-
Electrical Equipment"; Phase II, Vol II(U) and II(S), Boeing Report-D180-20186-4, Naval Air Systems Command, Contract N00019-76-C-0497; 1977.

23. Wallace, B.J., et al; "Composite Forward Fuselage Systems Integration"; Volume II, Technical Report AFFDL-TR-78-110; September 1978.

24. Zeitler, R.T. and Droste, C.S.; "Flight Control System Lightning Susceptibility Test Report"; General Dynamics Report TIS GA4013, No. 16PR623 Revision A; March 1979.

25. Burrows, B.J.C., et al; "A Comparison of Low-Level Swept CW and High-Level Transient Current Injection Testing on Full-Size Aircraft with Graphite Epoxy Panels"; IEEE International Symposium on Electromagnetic Compatibility; 1981.

26. Hewitt, Jr., R. P., Koo, F.H., Keys, D.;"Test and Evaluation of Graphite/Epoxy Composite Structure"; Martin Mairetta Aerospace Orlando FL; U.S. Army Materials and Mechanics Research Center Report AMMRC-TR-79-39; July 1979.

27. Walen, D. and Cooley, W.; "Atmospheric Electricity Hazards Vulnerability Test and Assessment"; (Draft Document) AEHP Program; April 1984.

A.5 Analytical Models

28. Williams, J.W. and Simpson, L.T.; "Preliminary Report of Finite-Difference Calculations of Simulated Lightning Response for the ALCM and F-16 Mockup", MRC Report AMRC-R-434, December 1982.

29. Naval Air System Command, U.S. Department of the Navy; "Electromagnetic Coupling Calculations on an Advance Composite and Metal F-14 Fighter Aircraft"; AIR-518-12; January 1982.

30. Eriksen, F.J., Rudolph, T.H., Perala, R.A.; "Atmospheric Electricity Hazards Analytical Model Development and Application"; AF Wright Aeronautical Laboratories Report AFWAL-TR-81-3084, Vol. III; August 1981.

31. Cooley, W.W., Mahaffey, D.W., and Rudzitis, A.; "DNA Prempt Program Communication Facility EMP Response - Prediction Techniques"; IEEE International Symposium on EMC; August 1977.

32. Cooley, W.W.; "EMP Facility Response Predictions-AECo AUTOVON Results"; DCA/DNA/USAF Working Group for HEMP testing of C3 Facilities; August 1976.

33. Cooley, W.W.; "EMP Response Prediction Techniques"; Inter-System Communications/Electronics for Contributing Scientists and Engineers; July 1974.

34. Cooley, W.W.; "Shielding Effectiveness of Non-Uniform Enclosures"; GEC Transactions, Vol. EMC-10, No. 1; March 1968.

35. Silvester, P., Modern Electromagnetic Fields, Prentice-Hall, Inc., 1968.

A.6 Design Guides/Specifications

36. Naval Air Systems Commmand; "Airframe Electrical Grounding Requirements Program" Final Report-AD-A115-06418; Vol. 1; February 1981.

37. Sommer, D.L.; "Protection of Electrical Systems from EM Hazards - Design Guide", Boeing Military Airplane Co.; AFWAL-TR-81-2118; September 1981.

38. Dunbar, W.G.; "High Voltage Design Guide"; Vol. V. Spacecraft; Boeing Aerospace Co.; AFWAL-TR-82-2057 Vol-5; January 1983.

39. Chamis, C.C.; "Design Concepts for Low-Cost Composite Engine Frame"; NASA Report NASA-TM-83544; 1983.

APPENDIX B

RESISTANCE MODELS FOR FASTENERS IN COMPOSITE MATERIAL

This appendix describes in detail the modelling methods used to obtain the resistance of metal fasteners in composite panels. The geometry used in the analyses is shown in Figure B-1. The problem to be solved is to calculate the resistance of the fastener attached to a composite panel where current flows from one edge of the panel through the panel and out the fastener (or vice versa). An equivalent problem is to consider a voltage or charge source at the fastener location and solve for the potential and therefore the electric field and current flow with appropriate boundary conditions at the edges of the panel. The current flow paths and equipotential lines are illustrated in Figure B-2. By obtaining the total electric field at the panel edge, the total current flowing through the panel can be calculated and then the total resistance of the fastener in the panel. The resistance, R, is calculated from Ohm's law, equation (1).

(1) $R = Vo / I$

where Vo = potential at fastener

$$I = \int_{-W/2}^{+W/2} E_x \cdot \sigma T \, dY$$

$$E_x = -dV/dX$$

and σ = conductivity

T = panel thickness

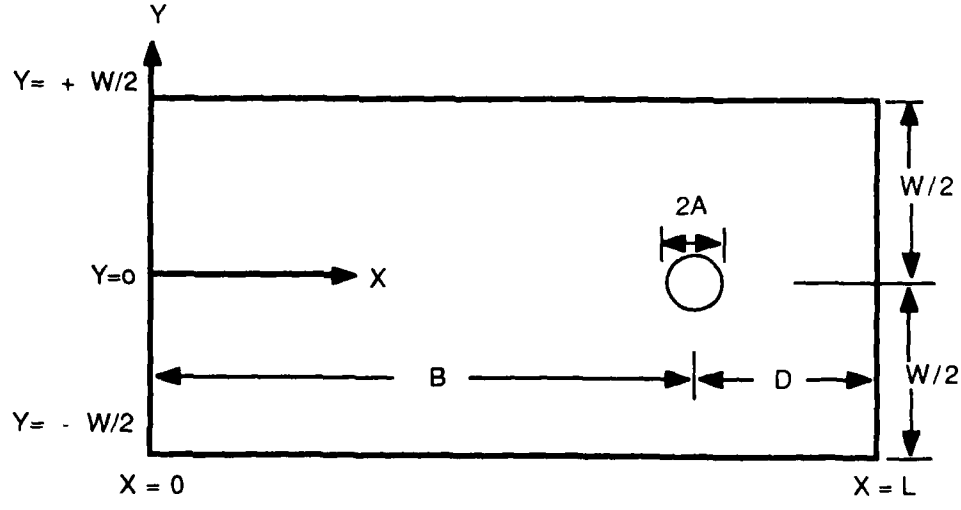

FIGURE B-1. GEOMETRY OF FASTENER IN PANEL

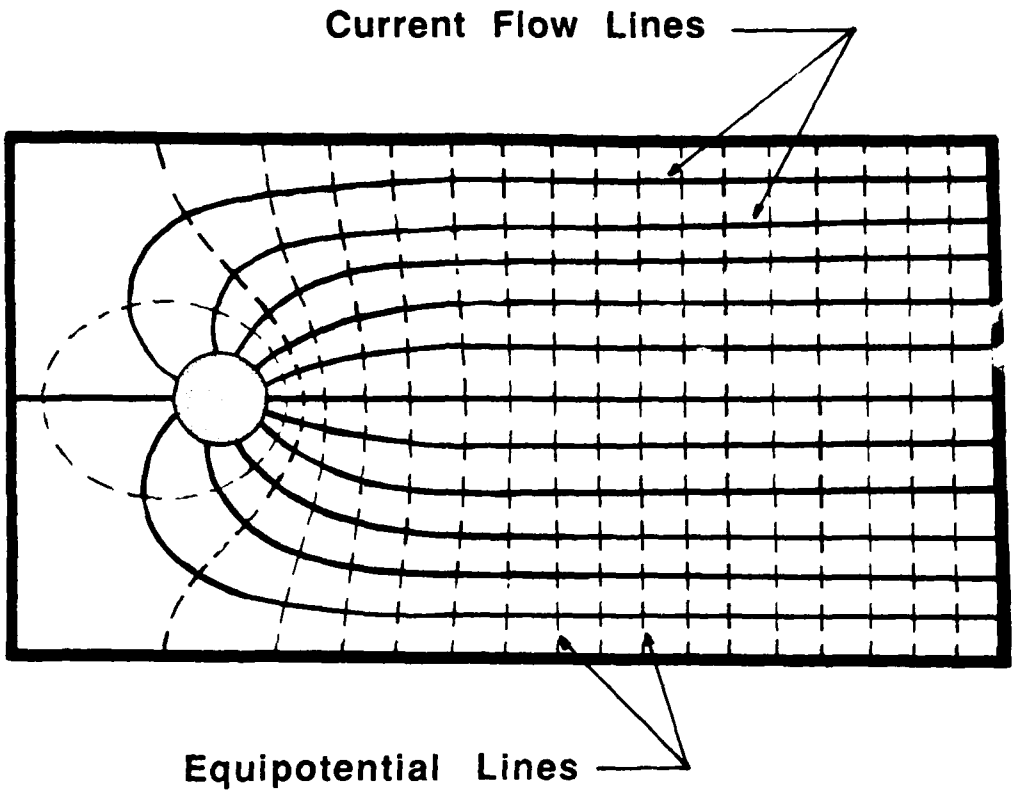

FIGURE B-2. EQUIPOTENTIAL AND CURRENT FLOW LINES OF A FASTENER IN A TEST PANEL

Ex is the electric field at X = 0 and is obtained from the potential, V, at the panel edge using the various methods described below. These methods include:

1. Green's function solution of Poisson's equation,
2. Numerical relaxation solution of Poisson's equation,
3. Method of images, one dimension,
4. Method of images, two dimensions.

Green's Function Solution

To solve for the potential at the panel edge, the solution for the potential on the entire panel must be found. The potential satisfies Poisson's equation with a voltage source located at the fastener. To use the Green's function method of solution the source is assumed to be a point source located at the fastener center. This limits these solutions to fasteners with dimensions small compared to the panel dimensions. Panel dimensions ten times larger than the fastener diameter should produce accurate results. Poisson's equation with a point source, Q, at X=B and Y=0 is given in equation (2).

$$(2) \qquad \nabla^2 V = Q \cdot \delta(X-B) \cdot \delta(Y)$$

The appropriate boundary conditions for the panel are:

$$V = 0 \qquad \text{at} \quad X = 0$$

$$\partial V/\partial X = 0 \qquad \text{at} \quad X = L$$

$$\partial V/\partial Y = 0 \qquad \text{at} \quad Y = \pm W/2$$

These boundary conditions correspond to current flowing from the fastener out the panel edge at X = 0 which is at a constant potential.

The Green's function method solves equation (2) by first solving the related eigenfunction equation (3)

$$(3) \qquad [\nabla^2 + K^2_n]\, \psi_n = 0$$

The Green's function for the problem can then be written

$$(4) \qquad G(R,R') = \sum_{n=0}^{\infty} \frac{\psi_n(R) \cdot \psi_n^*(R')}{K^2_n}$$

and the potential is then given by

$$(5) \qquad V(R) = \int G(R,R') \cdot \rho(R')\, dR$$

$$\rho(R') = Q \cdot \delta(X-B) \cdot \delta(Y)$$

The solution of the eigenvalue equation (3) which satisfies the above boundary conditions is

(6) $$\Psi_{mn} = A_{mn} \, \text{SIN} \, (2n+1)\pi X/2L \cdot \text{COS} \, 2m\pi Y/W$$

where
$$A_{mn} = \begin{cases} 2/\sqrt{LW} & m \neq 0 \\ \sqrt{2}/\sqrt{LW} & m = 0 \end{cases}$$

and $$K^2_n = \pi^2 \cdot [((2n+1)/L)^2 + 16m^2/W^2]/4$$

This results in the following form for the Green's function.

(7)
$$G(R,R') = \frac{32L}{\pi^2 W} \sum_{n=0}^{\infty} \text{SIN} \, (2n+1)\pi X/2L \cdot \text{SIN} \, (2n+1)\pi X'/2L \cdot \left[\frac{1}{(2n+1)^2} + 2 \cdot \sum_{m=1}^{\infty} \frac{\text{COS} \, 2\pi mY/W \cdot \text{COS} \, 2\pi mY'/W}{(2n+1)^2 + 16m^2 L^2/W^2} \right]$$

Then using equation (5) to solve for the potential gives

(8)
$$V(R) = \frac{V_o \sum_{n=0}^{\infty} \text{SIN} \, (2n+1)\pi X/2L \cdot \text{SIN} \, (2n+1)\pi B/2L \cdot \left[\frac{1}{(2n+1)^2} + 2 \cdot \sum_{m=1}^{\infty} \frac{\text{COS} \, 2m\pi Y/W}{(2n+1)^2 + 16m^2 L^2/W^2} \right]}{\sum_{n=0}^{\infty} \text{SIN}^2 \, (2n+1)\pi B/2L \cdot \left[\frac{1}{(2n+1)^2} + 2 \cdot \sum_{m=0}^{\infty} \frac{1}{(2n+1)^n + 16m^2 L^2/W^2} \right]}$$

Differentiating the potential at x=0 and integrating across the panel edge at x=0 gives the total current flowing through the panel relative to the applied voltage as given in equation (9). This can then be used to find the fastener resistance in the panel using equation (1) for the resistance.

(9)
$$\frac{I}{\sigma T} = \frac{-V_o \pi W}{2L} \frac{\sum_{n=0}^{\infty} [1/(2n+1)] \cdot \text{SIN} \, (2n+1)\pi B/2L}{\sum_{n=0}^{\infty} \text{SIN}^2 \, (2n+1)\pi B/2L \cdot \left[\frac{1}{(2n+1)^2} + 2 \sum_{m=1}^{\infty} \frac{1}{(2n+1)^2 + 16m^2 L^2/W^2} \right]}$$

To obtain quantitative results, the infinite sum in equation (8) is used in a computer code and enough terms are included so the sum remainder is small. For this calculation at the edge of the panel the sum converges fairly quickly, less than twenty terms for the parameters considered here. The convergence is not as good for determining potential at any point on the panel.

Numerical Relaxation

The second technique of solving Poisson's equation using the above boundary conditions is using a numerical relaxation technique. The specific technique used here is the Liebmann iteration method given by Silvester (1968) p. 56-65. The basis for this approach is to calculate potentials at selected grid points using the finite difference form of Laplace's equation and to set source grid points equal to the applied voltage. The finite difference form of Laplace's equation (for Res=0) at grid point I,J is

(10) V(I,J+1)+V(I,J-1)+V(I+1,J)+V(I-1,J)-4*V(I,J) = Res

The relaxation technique involves initially assuming values for V(I,J) at all grid points. Equation (10) is then equal to some finite residue at each grid point. Liebmann's iteration technique involves calculating one residue at a time and readjusting the potential value at that point by using

(11) V(new) = V(old) + a*Res/4

where a = overrelaxation factor with a=1 to 2. Best convergence is usually obtained for a between these values. Res is the residue calculated at the grid point being examined using equation (10). Each grid point in the considered geomtry to be solved is iterated until the calculated residues at each point are less than some predetermined maximum. The more accurately the inital guess for the voltage distribution, the faster the convergence.

The boundaries and other points which are at a predetermined voltage are not changed in this process. So for the fastener analysis, the grid points representing the fastener are set equal to Vo and at the panel edge at x=0 the potential is set to zero.

This technique for determining the voltage allows for finite size fasteners. The size of the fasteners is limited by the grid spacing size. This technique is more appropriate for larger fasteners in composite panels than the Green's function technique. This technique gave good results consistent with the Green's function technique and the resistance paper measurements. A sample basic program for a fastener in the middle of a panel is given in Figure B-3.

Method of Images - 1-Dimension

The method of images solves Poisson's equation by assuming a set of voltage source images outside the region of interest (in this case outside the panel) which allow the boundary conditions to be satisified. For the one dimensional image technique the geometry used is shown in Figure B-4. The panel is assumed to be infinitely long with boundaries only at x=0 and x=L. This technique obviously is accurate only for long thin panels. The number of images needed to satisfy the boundary conditions at the edges is infinite.

To calculate the electric field at x=0, the image sources are paired up for summation. The electric field strength decreases as the square of the distance of the source to the x=0 plane so the summation can be terminated when additional source image terms become small. The electric field at x=0

```
10 REM: SAMPLE LIEBMANN ITERATION PROGRAM
20 REM: FASTENER IN CENTER OF PAPER IN X DIRECTION
30 REM V=0 ALONG Y=0: E PARALLEL ALONG OTHER EDGES =0
40 REM CALCULATES POTENTIAL, RESISTANCE OF SHEET AND FASTENER
50 ALPHA = 1.5:VO=10:NMX=30
60 DX=.5:DY=DX:REM USE SQUARE GRID
70 W=3:D=1.1:B=5!:A=.06:REM DIMENSIONS IN INCHES
80 SG=28000:T=.056:T=T*.0254
90 NX=INT(W/2/DX+1.5):NY=INT((B+D)/DY+1.5)
100 IFAS=INT(B/DY+1.5):REM POSITION OF FASTENER
110 NIF=INT(A/DX+.5):REM NUMBER OF POSITIONS FOR FASTENER
120 PRINT "NX=";NX;"   NY=";NY;"   IFAS=";IFAS;"  NIF=";NIF
130 RSMAX=.0025
140 DIM V(NY,NX)
150 FOR I =1 TO NY
160 FOR J=1 TO NX
170 V(I,J)=VO/2
180 NEXT:NEXT
190 FOR J=1 TO NX
200 V(1,J)=0
210 NEXT
220 V(IFAS,1)=VO
230 KOUNT=0
240 R=ALPHA/4
250 I1=INT(.2*IFAS-NIF+.5):I2=IFAS
260 REM: ITERATION CYCLE
270 INDIC=0:M1=0:M2=0:MR=0
280 FOR I=2 TO NY-1
290 IF I=IFAS THEN GOTO 350
300 RES=2*V(I,2)+V(I-1,1)+V(I+1,1)-4*V(I,1)
310 AR=ABS(RES):IF I=I1 THEN M1=AR:IX1=1:IY1=I
320 IF MR<AR THEN MR=AR:IX=1:IY=I
330 IF AR>=RSMAX THEN INDIC=1
340 V(I,1)=V(I,1)+R*RES
350 RES=V(I,NX-1)+V(I-1,NX)+V(I+1,NX)-3*V(I,NX)
360 AR=ABS(RES):IF I=I2 THEN M2=AR:IX2=NX:IY2=I
370 IF AR=>RSMAX THEN INDIC=1
380 V(I,NX)=V(I,NX)+R*RES:IF MR<AR THEN MR=AR:IX=NX:IY=I
390 V(IFAS,1)=VO
400 IF NIF>0 THEN GOTO 910
410 FOR J=2 TO NX-1
420 RES=V(I,J+1)+V(I,J-1)+V(I-1,J)+V(I+1,J)-4*V(I,J)
430 AR=ABS(RES):IF MR<AR THEN MR=AR:IX=J:IY=I
440 IF AR=>RSMAX THEN INDIC=1
450 V(I,J)=V(I,J)+R*RES
460 NEXT J
470 NEXT I
480 FOR I=2 TO NX-1
490 RES=V(NY-1,I)+V(NY,I-1)+V(NY,I+1)-3*V(NY,I)
500 AR=ABS(RES):IF MR<AR THEN MR=AR:IX=I:IY=NY
510 IF AR=> RSMAX THEN INDIC=1
520 V(NY,I)=V(NY,I)+R*RES
530 NEXT
540 RES=V(NY,NX-1)+V(NY-1,NX)-2*V(NY,NX)
550 AR=ABS(RES):IF MR<AR THEN MR=AR:IX=NX:IY=NY
```

FIGURE B-3. LIEBMANN ITERATION CODE

```
560 V(NY,NX)=V(NY,NX)+R*RES
570 RES=V(NY-1,1)+V(NY,2)-2*V(NY,1)
580 AR=ABS(RES):IF MR<AR THEN MR=AR:IX=1:IY=NY
590 V(NY,1)=V(NY,1)+R*RES
600 KOUNT=KOUNT+1
610 PRINT KOUNT;" ";M1;IX1;IY1;M2;IX2;IY2;MR,IX,IY
620 IF KOUNT=>NMX THEN GOTO 640
630 IF INDIC=1 THEN GOTO 270
640 REM: EXIT ROUTINE
650 REM: SET EPSON PRINTER FOR COMPRESSED PRINT & 25/72 IN. LINES
660 REM LPRINT CHR$(15),CHR$(27)"A"CHR$(25)
670 FOR JJ=1 TO NY
680 FOR KK=1 TO NX
690 J=NY-JJ+1:K=NX-KK+1
700 PRINT USING " #.##"; V(J,K);
710 REM LPRINT USING "  #.##"; V(J,K);
720 NEXT
730 PRINT:PRINT
740 REM LPRINT
750 NEXT
760 PRINT
770 PRINT KOUNT;"  ITTERATIONS WITH OVERRELAXATION FACTOR ";ALPHA
780 REM CALCULATE CURRENT ON V=0 EDGE AND RESISTANCE OF SHEET
790 ET=0
800 FOR I=1 TO NX
810 E=V(2,I)-V(1,I)
820 PRINT "X,E";(I-1)*DX;E/DX
830 NN=2:IF I=1 THEN NN=1
840 ET=ET+E*NN:NEXT I
850 JT=SG*T*ET:R=VO/JT
860 PRINT "W=";W;"  D=";D;"  B=";B;"  A=";A
870 PRINT "RESISTANCE OF SHEET=";R
880 RS=(B-A)/W/SG/T:REM RESISTANCE OF SHEET WITH PARALLEL EDGES
890 RF=R-RS:PRINT "FASTENER RESISTANCE=";RF
900 END
910 REM: FOR FINITE SIZE FASTENER, A>=DX
920 FOR K=1 TO NIF
930 V(IFAS,K+1)=VO
940 V(IFAS+1,1)=VO
950 V(IFAS-1,1)=VO
960 NEXT K
970 GOTO 410
```

for pairs of image sources is given by equations (12) and (13).

$$(12) \quad E_{2n}(y) = \frac{2 V_o (-1)^{n-1}}{\ln(a/2/x_{2n})} \cdot \frac{x_{2n}}{r_{2n}}$$

$$(13) \quad E_{2n+1}(y) = \frac{2 V_o (-1)^{n}}{\ln(a/2/x_{2n+1})} \cdot \frac{x_{2n+1}}{r_{2n+1}}$$

where $x_{2n} = (2n-1)B + 2nD$

$x_{2n+1} = (2n+1)B + 2nD$

$r_o^2 = x_o^2 + y^2$

The electric field is then integrated along the y axis as given in equation (1). The results from this method are surprisingly good considering the one dimensional approximation.

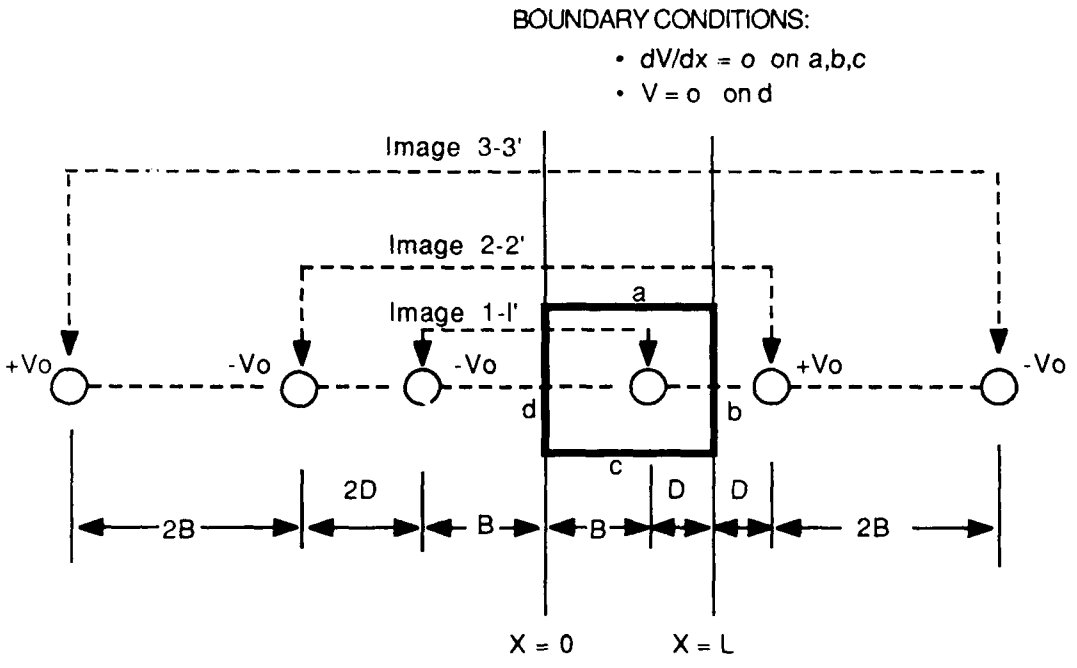

FIGURE B-4. IMAGE SOURCES FOR 1-D METHOD OF IMAGES

Method of Images - 2 - Dimensional

The two dimensional method of images was the most inconsistent method tried in these analyses. The problem comes from the lack of convergence of the electric field due to the images. The set of images for the two

dimensional approach is shown in Figure B-5. As in the one dimensional case there are an infinite set of images required to satisfy the boundary conditions. In this case, however, the number of images increases rapidly away from the point of calculation. The electric field decreases proportional to the square of the distance from the calculation point, however, the number of images increases fast enough to yield nonconvergent results.

The best approach using the two dimensional image theory after many different types of pairing of terms resulted from just using the four image sources closest to the panel. The expressions for the electric field at x=0 are similar to that given for the one dimensional case. The results from this method are not in very good agreement with the other methods. This is due to the nonconvergence of the method.

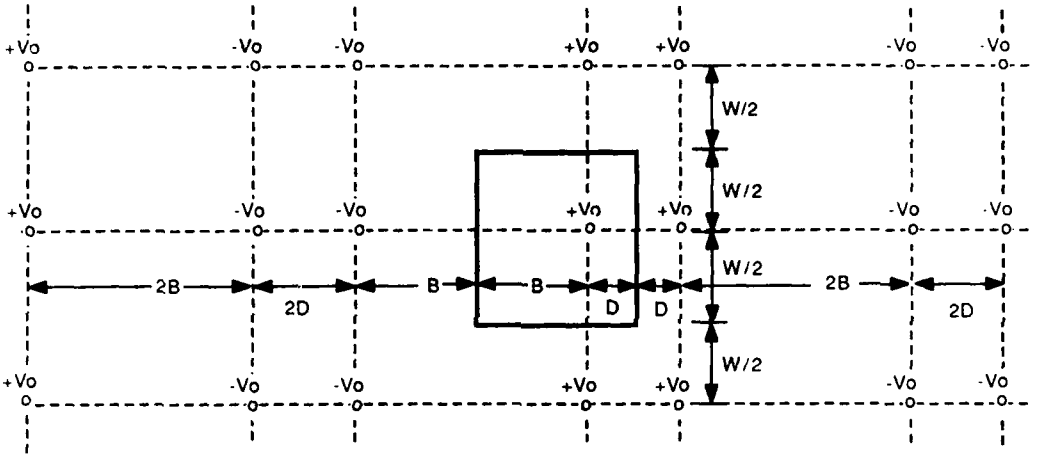

FIGURE B-5. IMAGE SOURCES FOR 2-D METHOD OF IMAGES

APPENDIX C

DISTRIBUTION LIST

Civil Aviation Authority (5)
Aviation House
129 Kingsway
London WC2B 6NN England

Embassy of Australia (1)
Civil Air Attache
1601 Mass. Ave. NW
Washington, DC 20036

Scientific & Tech. Info FAC (1)
ATTN: NASA Rep.
P.O. Box 8757 BWI Airport
Baltimore, MD 21240

Northwestern University (1)
Trisnet Repository
Transportation Center Library
Evanston, ILL 60201

DOT-FAA AEU-500 (4)
American Embassy
APO New York, NY 09667

University of California (1)
Service Dept Institute of
Transportation Standard Lib
412 McLaughlin Hall
Berkely, CA 94720

British Embassy (1)
Civil Air Attache ATS
3100 Mass Ave. NW
Washington, DC 20008

Director DuCentre Exp DE LA (1)
Navigation Aerineene
941 Orly, France

ANE-40	(2)	ACT-61A	(2)	ASW-53B	(2)
ASO-52C4	(2)	AAL-400	(2)	AAC-64D	(2)
APM-13 Nigro	(2)	M-493.2 Bldg. 10A	(5)	ACE-66	(2)
AEA-61	(3)	APM-1	(1)	ADL-1	(1)
ADL-32 North	(1)	APA-300	(1)	ALG-300	(1)
AES-3	(1)	AGL-60	(2)	ACT-5	(1)
ANM-60	(2)				

FAA, Chief, Civil Aviation Assistance Group (1)
Madrid, Spain
c/o American Embassy
APO-New York 09285-0001

Al Astorga (1)
Federal Aviation
Administration (CAAG)
American Embassy, Box 38
APO-New York 09285-0001

Dick Tobiason (1)
ATA of America
1709 New York Avenue, NW
Washington, DC 20006

Burton Chesterfield, DMA-603 (1)
DOT Transportation Safety Inst.
6500 South McArthur Blvd.
Oklahoma City, OK 73125

FAA Anchorage ACO
701 C Street, Box 14
Anchorage, Alaska 99513

FAA Fort Worth ACO
P.O. Box 1689
Fort Worth, TX 76101

FAA Atlanta ACO
1075 Inner Loop Road
College Park, Georgia 30337

FAA Long Beach ACO
4344 Donald Douglas Drive
Long Beach, CA 90808

FAA Boston ACO
12 New England Executive PArk
Burlington, Mass. 01803

FAA Los Angeles ACO
P.O. Box 92007, Worldway Postal Center
Hawthorne, CA 90009

FAA Brussels ACO
% American Embassy, APO,
New York, NY 09667

FAA New York ACO
181 So. Frankline Ave., Room 202
Valley Stream, NY 11581

FAA Chicago ACO
2300 E. Devon, Room.232
Des Plains, Illinois 6008

FAA Seattle ACO
17900 Pacific Highway South, C-68966
Seattle, Washington 98168

FAA Denver
[illegible] East 20th Ave., Suite 307
[illegible], Colorado 80[illegible]

FAA Wichita ACO
Mid Continent Airport, Room 100 FAA Bldg.
1891 Airport Road
Wichita, KA 67209

Frank Taylor
3542 Church Road
[illegible] City, MD 21043

Dr. Hans A. Krakauer
Deputy Chairman, International Airline
Pilots Association Group
[illegible]
[illegible], Portugal

[illegible]
[illegible] St.
Springfield, VA 22152

Geoffrey Lipman
Executive Director, President du Conseil
International Foundation of Airline
Passenger Associations
Case Postale 462, 1215 Geneve
15 Aeroport, Suisse, Geneva

[illegible] Earl F. Livingston, Jr.
Director, Aerotech Operations for
the IAPA Group
1505 Crystal Drive, Suite 1112 South
Arlington, VA 22202

APPENDIX

DISTRIBUTION LIST

Nickolus O. Rasch
AWS-122
FAA Headquarters
800 Independence Ave.
Washington, DC 20591

Dayton O. Curtis, ANM-100A
Anchorage ACO
Federal Aviation Administration
701 C Street, Box 14
Anchorage, Alaska 99513

Barry D. Clements
Aircraft Certification Division,
ACE-100
FAA Central Region Headquarters
601 East 12th Street
Kansas City, Missouri 64106

Gerald Mack
Aircraft Cetification Office,
Federal Aviation Administration
1075 Inner Loop Road
College Park
Atlanta, Georgia 30337

Walter F. Horn
Aircraft Certification Office, ACE
Federal Aviation Administration
2300 East Devon (Room 232)
Des Plaines, Illinois 60018

Robert A. Gambrill, Jr.
Aircraft Certification Office, ACE
Federal Aviation Administration
FAA Building, Room 100
1801 Airport Road,
Wichita, Kansas 67209

Jack Sain
Manager, Aircraft Certification
Division, ANE-100
Federal Aviation Administration
12 New England Executive Park
Burlington, Massachusetts 01803

Ray Borowski
New York Aircraft Certification
Office, ANE-173
181 South Franklin Ave. (Room 202)
Valley Stream, New York 11581

Leroy A. Keith
Manager, Aircraft Certification
Division, ANM-100
Northwest Mountain Region Headquarters
Federal Aviation Administration
17900 Pacific Highway South, C-68966
Seattle, Washington 98168

Sam Frick, ANM-140L
Los Angeles ACO
Federal Aviation Administration
4344 Donald Douglas Drive
Long Beach, California 90809

Herb Peters, ANM-173W
Los Angeles ACO
Federal Aviation Administration
Post Office Box 92007
Los Angeles, California 90009

Woodford R. Boyce, ANM-100D
Aircraft Certification Office
Federal Aviation Administration
10455 East 25th Avenue, Suite 307
Aurora, Colorado 80010

[illegible] P. Watson, ASW-100
Aircraft Certification Division
Federal Aviation Administration
[illegible]thwest Region Headquarters
Box 1689
[illegible], Texas 76101

Jim Treacy, ANM-103N
Aircraft Certification Division
Northwest Mountain Region Headquarters
Federal Aviation Administration
17900 Pacific Highway South, C-68966
Seattle, Washington 98168

Gene Vandermolen, ANM-111
Federal Aviation Administration
Northwest Mountain Region Headquarters
17900 Pacific Highway South C-68966
Seattle, WA 98168

Richard Vaughn, ASW-111
Federal Aviation Administration
Southwest Region Headquarters
Post Office Box 1689
Fort Worth, Texas 76101

Don Whiston, ACE-130C
Federal Aviation Administration
2300 E. Devon Avenue (Room 240)
Des Plaines, Chicago Ill. 60018

Peter Cuneo, ANE-173
Federal Aviation Administration
New York ACO
181 So. Franklin Avenue (Room 202)
Valley Stream, New York 11581

Hal Foland, ACE-111
Federal Aviation Administration
Central Region Headquarters
601 East 12th Street, Federal Bldg.
Kansas City, MO 64106

Ron Vavruska, ANE-153
Federal Aviation Administration
New England Region Headquarters
12 New England Executive Park
Burlington, Mass. 01803

ASF-1 - Office of Aviation Safety

AST-1 - Office of Science & Advanced Technology

APM-1 - Program Engineer & Maintenance Service

AVS-1 - Associate Administrator for Aviation Standards

AWS-1 - Office of Airworthiness

AWS-100 - Aircraft Engineering Division

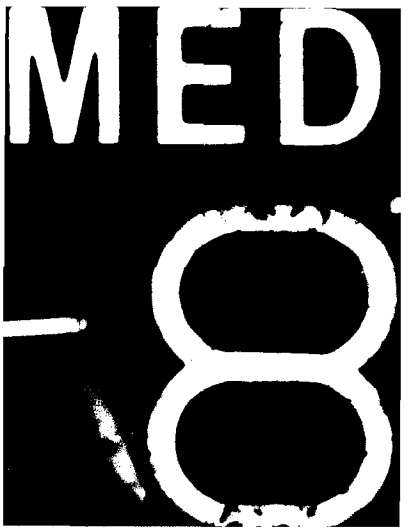
MED
8